Solar Energy 208 (2020) 493–514

Contents lists available at ScienceDirect

Solar Energy

journal homepage: www.elsevier.com/locate/solener

Daylight autonomy improvement in buildings at high latitudes using horizontal light pipes and light-deflecting panels

Biljana Obradovic [a,b,*], Barbara Szybinska Matusiak [a]

[a] Norwegian University of Science and Technology, NTNU, Norway
[b] Norconsult AS, Norway

ARTICLE INFO

Keywords:
Laser-cut panel (LCP)
Horizontal light pipe
Daylight tube
Daylight autonomy (DA)
High latitude
Low solar altitude
Overcast sky

ABSTRACT

Horizontal light pipes (HLP) have shown the potential to convey daylight deeper into buildings. The wide variation in incident angles of sunlight rays and the resulting numerous interreflections of light rays within the pipe are the main reasons for the limited light transmittance of such light pipes during certain daylight periods. This paper presents a research study on different configurations of acrylic laser-cut panels (LCP) applied at the entrance of horizontal pipes as light collectors to increase the transmittance of HLPs and improve daylight autonomy in spaces equipped with HLPs. This study required the development of a suitable methodology. The study begins with an experimental laboratory test of a HLP scale model to determine the light transmittance efficiency (standard daylight guide characteristic) of HLPs with several LCP configurations. The results from the laboratory test are combined with the statistical data for both the direct and diffuse illuminance on the vertical south-oriented surface (Satel-Light database) for the location selected for the analyses (Oslo, Norway). The analyses are discussed via the application of a theoretical model of an office space equipped with a HPL as well as through the concept of daylight autonomy (DA) in an indoor space. The paper shows that a certain static LCP configuration has the potential to increase DA_{100} and DA_{300} to 10% and 19%, respectively, at a 2.1 m distance from the façade, and 8.75% and 16%, respectively, at a 4.5 m distance. This paper also contributes to lighting science with its data on the light transmittance efficiency of each LCP configuration, which can be applicable in further research.

0. Nomenclature

T	Light transmission efficiency factor for light pipe and a certain light incident ray
TTE	Light transmission efficiency factor for light pipe for overcast sky conditions
L	Length of light pipe, meters
D_p	Diameter of light pipe, meters
p	Aspect ratio of light pipe (p = length/diameter of light pipe)
R	Reflectance factor of inner surface of light pipe
D/W	Distance-to-width ratio of Laser-Cut panel
θ	Angle of the cuts on the Laser-Cut panel, degrees
Al, Az	Solar altitude and azimuth, degrees
αl, αz	Light incident angle of solar altitude and azimuth on certain surface, degrees
r_2	Angle at which deflected light ray leaves the exit face of the Laser-cut panel, degrees
β	Tilt/rotating angle of LC-panel relative to pipe's entrance plane, degrees
$E_{direct}(ZERO)$, $E_{diffuse}(ZERO)$	Direct or diffuse illuminance measured at the tube's entrance, lux
$E_{direct}(BaseCase)$, $E_{diffuse}(BaseCase)$	Illuminance measured on the tube's exit without LCP configuration, lux
$E_{direct}(T\text{-}R^*)$, $E_{diffuse}(T\text{-}R^*)$	Illuminance measured at the tube's exit for certain LCP configuration*, lux
Es_{direct}, $Es_{diffuse}$	Direct or diffuse illuminance on a vertical south façade developed from the Satel-Light, lux
$Er_{direct}(T\text{-}R^*)$, $Er_{diffuse}(T\text{-}R^*)$	Direct or diffuse real expected illuminance at the tube's exit for a certain LCP configuration*, lux
$\eta_{direct}(T\text{-}R^*)$, $\eta_{diffuse}(T\text{-}R^*)$	Standard daylight guide characteristic for direct or diffuse light
Er (T-R*)	Total real expected illuminance at the tube's exit for a certain LCP configuration, lux
δ	Beam spread of the curved reflector at the exit of the light pipe in the theoretical model, degrees

(continued on next column)

(continued)

(continued on next page)

* Corresponding author.
E-mail addresses: Biljana.obradovic@norconsult.com, Biljana.obradovic@ntnu.no (B. Obradovic).

https://doi.org/10.1016/j.solener.2020.07.074
Received 20 April 2020; Received in revised form 22 July 2020; Accepted 23 July 2020
Available online 14 August 2020

(*continued*)

Ω	Solid angle of the curved reflector at the exit of the light pipe in the theoretical model, steradian
P	Areal of the light pipe's exit in the theoretical model, square meters
E_1, E_2	Required light illuminance on the light pipe's exit and the reference surface
Φ_1	Required light flux at the light pipe's exit, lumen
I_2	Required light intensity on the reference surface in a theoretical model, candela
A	Areal of the reference surface, square meters
d	Mounting height of the tube above the workplane, meters

*For all of the LCP configurations, see Tables 6 and 7.

1. Introduction

To fulfil new legislation requirements (such as *TEK17* or *NS3700* in Norway, where this study was conducted), buildings have become more compact, which results in spaces inside the buildings lacking natural light (Houck, 2015). This drawback has been noted, and some concepts of integrative lighting (light for the circadian rhythm) have been used to mitigate it; however, research and practice have still not come to a successful solution (Chinazzo et al., 2020; Perez et al., 2018; Yuda et al., 2017). The initial concept of finding a sustainable solution for the lack of daylight inside buildings has been additionally overshadowed by the decreasing costs of LED lighting (Herring, 2006).

Moreover, regulations on the daylight factor (D) are becoming stricter. A daylight factor demand of $D_{mean} > 2\%$ for permanently occupied rooms is becoming difficult to achieve, as buildings simultaneously follow stricter energy efficiency demands, with a 30% increase of wall thickness and a 25% decrease in the light transmission of window glazing (Ulimoen et al., 2020).

The new European standard, *EN-17037 Daylight in Buildings*, brings a requirement of 50% of daylight hours during the year, with daylight provision of a minimum of 300 lx for 50% of the area and 100 lx for 95% of the area (Mardaljevic et al., 2013). Daylight provision refers to the level of illuminance achieved across a fraction of a reference plane for a fraction of daylight hours. Daylight hours in this standard refers to the time from sunrise to sunset. This means at least six hours of 300 lx of daylight on average throughout the year, which occurs between 7 AM and 5 PM (the occupancy period of a typical office space).

As global economic growth forces centralization, the most intensive development of commercial buildings takes place in city centres, where high land prices lead to high-rise buildings. Multi-floor buildings have large facade areas that are predominantly made of glass and steel (Yeang and Powell, 2007). Glass facades, besides daylighting, provide unwanted glare and solar heat. Both research and post-occupancy reviews have shown that visual discomfort forces users to manually control sunscreens (Galasiu et al., 2004; Lindsay and Littlefair, 1992; Rea, 1984; Rubin et al., 1978). Especially in areas at higher latitudes, the conditions of clear sunny skies are not immediately connected with positive daylighting effects, since low solar altitude brings about glare and overheating issues. Automated sun-shading is, according to the practice in Scandinavia, pulled down and closed at a threshold of 43,000 lx on a façade and not pulled up before illuminance decreases under 23,000 lx (Christoffersen and Johnsen, 1999; Johnsen et al., 2011). Manually controlled sun-shading remains in a closed position much longer after the critical excessive light situation ends, usually until the user opens them again. A study by Reinhart (2004) showed that the initial daylight level in an office, at the time a user arrives, psychologically and physiologically determines their lighting comfort and need for electrical light. Such facts help note that low daylight level in an office, either as a result of the manual adjustment of sunscreens the previous day or the room's orientation and lack of sunlight, will increase the psychological need for a higher level of artificial light.

A literature review on daylight transport systems (DTS) revealed that light pipes can reduce the energy used for electrical lighting in commercial buildings at higher latitudes by up to 30% (Courret et al., 1998; Garcia Hansen and Edmonds, 2003; Kwok and Chung, 2008; Mayhoub, 2011; Obradovic and Matusiak, 2019). As electrical energy for lighting

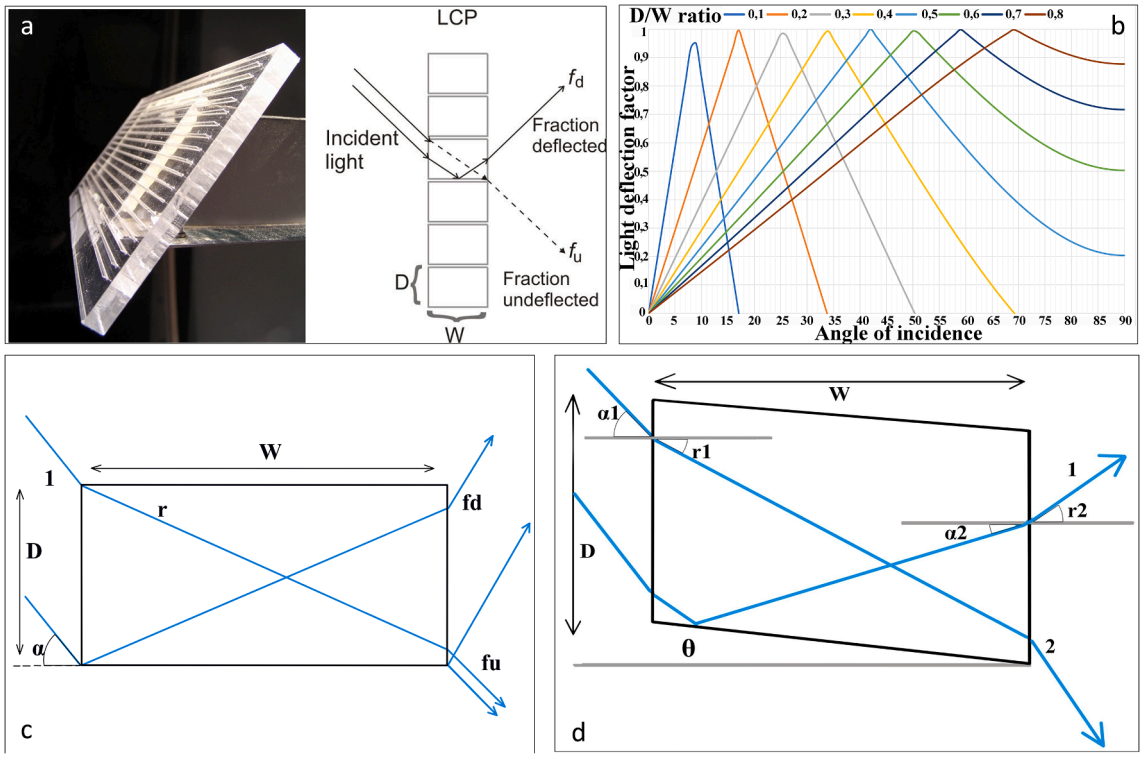

Fig. 1. (a) Laser-cut panel (Garcia Hansen et al., 2009); (b) Light deflection factor for D/W ratios for Edmond's LCP design (Weibye and Matusiak, 2019); (c) Light deflection principle in non-angled LCP; (d) Light deflection principle in angled LCP.

in commercial buildings in Norway accounts for 40% (Kolås, 2011) of total building energy used, the fact that a reduction of a 30% could give a total energy reduction of 12% is important. According to the Norwegian standard *SN/TS 3031:2016 Energy Performance of Buildings—Calculation of Energy Needs and Energy Supply* and the European standard *EN 15193-1:2017 Energy Performance of Buildings—Energy requirements for Lighting (Part 1: Specifications, Module M9)*, the maximum 145 kWh/m^2 per year is allowed for commercial buildings in energy class C, while the maximum of 115 kWh/m^2 enables energy class B. The stricter class is characterized by a 20% energy reduction, a significant part of which can be accomplished by reducing the need for electrical lighting.

The need for reliable and prolonged daylight autonomy, especially during the mornings and afternoons, is directly related to the energy requirements of buildings that rely on electrical energy generated from PV panels. The peak load for energy consumption in commercial buildings starts sharply at 7 AM and remains linear until 5 PM, while the peak of solar energy generation follows suns alignment with the south (Lindberg et al., 2019). Prolonged daylight autonomy could have an impact on the balance energy management of buildings in terms of the fact that 40% of the energy consumption in commercial buildings is used for artificial lighting.

Many post-occupancy reviews has shown that light controlling systems with light sensors integrated in the ceiling to screen daylight levels on the working surface do not work as they should. The reason for this is a drastical decrease of daylight level from the side window and deeper in the space (Kolås, 2011). Some recent studies conducted in higher latitude areas have proposed sun-screening and daylighting elements suitable to deal with low solar altitude issues (visual and thermal comfort simultaneously), but their implementation in real projects has been delayed and hindered by many decisions and issues (Arnesen et al., 2011; Kolås, 2013). If a certain daylighting transport system could convey daylighting at more balanced levels, this could help the controlling system have more reliable operation and would result in easier decision-making regarding the placement of lighting sensors.

Daylight transport elements, such as light pipes, can be layered with mirror folium, aluminium, or silver, with a reflectivity (R) of 99%. The total light transmittance of the pipe, T, is defined as a direct function of reflectivity, R, where L is the pipe's length, D_p is the pipe's diameter, and α is the plane light incident angle relative to the light pipe's axis (Eq. (1)) (Zastrow and Wittwer, 1986, 1987). The light transmittance effectivity is in this case, beside the pipe's inner reflectance, highly dependent on the light incident angle.

$$T = R^{L\times tan\alpha \div D_p} \tag{1}$$

Light rays with an axillary incident angle to the pipe's axis, where no light rays inter-reflect along the pipe, contribute the most to the light transmission efficiency. Any increase in the incident angle increases the number of interreflections, and the total light transmittance of the pipe decreases simply because the inner surface is not 100% reflective.

In order to solve the problem of unfavourable (oblique) incident angles, several studies have used approach with deflected incident light. Light deflection panels, in this case Laser-Cut panels (LCPs), can deflect the incident light and, in turn, change its propagation direction. LCPs have been adopted as an effective light redirecting element in architecture since the development of the theory of light deflection in 90s (Edmonds, 1993), but the original idea dates to the very late nineteenth century (Wadsworth, 1903).

A laser-cut panel is produced by making parallel laser cuts in a transparent acrylic panel (Fig. 1a), where each cut becomes a "light reflective mirror". Fig. 1c illustrates the deflection mechanism in the case of straight cuts. The definition of light deflection on LCP states that "light is deflected in a rectangular prismatic element by refraction, total internal reflection and refraction again" and "an array of prismatic elements forms a light deflecting panel called a Laser-Cut Panel (LCP)" (Edmonds, 1993). Eqs. (2)–(4) explains how to calculate the outgoing angle of light, where the total angle through which the incident light is deflected is $\alpha_1 + r_2$ (see also Fig. 1d). For the $\theta = 0^\circ$ (angle of the cuts), the angle at which deflected light leaves the exit face, r_2, is the same as the angle of incidence on the panel, α_1. Edmond also explains that sloped laser-cuts have a higher deflecting factor for variating incident angles (span of angles) (Fig. 1d), but because of the technical impossibility of developing sloped cuts, there has not been any research addressing sloped cuts in the field of daylighting. The fraction of deflected light depends on the angle of incidence as well as the cut's distance-to-width ratio, D/W, which is defined with the help of a deflection factor (Fig. 1b).

$$\alpha_2 = r_1 - 2\theta \tag{2}$$

$$\mathrm{Sin}\alpha_1 = \frac{\sin r_1}{\mathrm{n}} \tag{3}$$

$$r_2 = \sin^{-1}(n \times \sin(r_1 - 2\theta) \tag{4}$$

LCPs have been used to enhance daylight collection or control excessive sunlighting. They have been used in skylights, windows, and awnings, in order to deflect incoming light and send it toward the indoor ceiling or to deflect it back to the outdoor space and screen the indoor space of solar radiation during the hottest time of day or year (Arnesen et al., 2011; Creda and Matusiak, 2017; Edmonds, 2005; Edmonds and Pearce, 1999; Freewan, 2014; Kischkoweit-Lopin, 2002; Knoop et al., 2016; Labib, 2013; Ruck et al., 2000; Weibye and Matusiak, 2019). Such studies conclude on the same fact that LCPs have the potential to deflect or disperse direct sunlight, reducing the need for blinds in the case of excessive sunlight.

A vertical pipe equipped with a single-sheet-, gable-, or pyramid-formed LCP, and through the idea of rotation, has been introduced in several studies (Edmonds et al., 1995; Garcia-Hansen and Edmonds, 2015; Garcia Hansen et al., 2009; Kadir et al., 2019). A recent study with rotating deflecting sheets showed the improvement of illumination and the temporal uniformity of illuminance on the pipe's exit (Venturi et al., 2006). The study concluded that the LCP can be used as an alternative to heliostats and sun-tracking systems. Meanwhile, a research study with vertical light pipes and LCPs in different tilts showed that the tilt of a LCP should be strongly developed according to the south-north orientation (Nair et al., 2015).

Horizontally placed light pipes, situated in the ceiling plenum, have shown many advantages over vertical light pipes, especially in multi-floored buildings. Several researches in the last decade have also shown the potential in applying an LCP as a deflector for non-axillary rays on horizontal light pipes (Garcia Hansen and Edmonds, 2003; Garcia Hansen et al., 2001; Kwok and Chung, 2008). The main objective in such studies was to improve the light collection of high-altitude light during noon, since those researches have been performed in the tropical climates of lower latitude locations.

This study exclusively examines horizontal cylindrical light pipes, relying on the solar microclimate of high latitude areas. The study addresses a gap in the research on LCPs by examining double/symmetrically rotated panels with vertical cuts for handling the variating azimuth. Moreover, this study consists of experimental parametric measurements and the theoretical analysis of daylight autonomy reported in daily and yearly hours in the inner space 2.1 and 4.5 m distances from the façade wall.

The paper is structured as follows: First, the Introduction establishes the research objective. The research on a whole consists of two parts that are explained in Section 2: Methodology. The research uses a local solar microclimate for the analyses presented in Section 3: Outdoor Daylight Accessibility. The fourth and fifth chapters present the method of the experimental and theoretical part of the study. The results are presented and explained in Section 6. The Discussion chapter explains the results in general, justifies the research hypotheses and importance of the

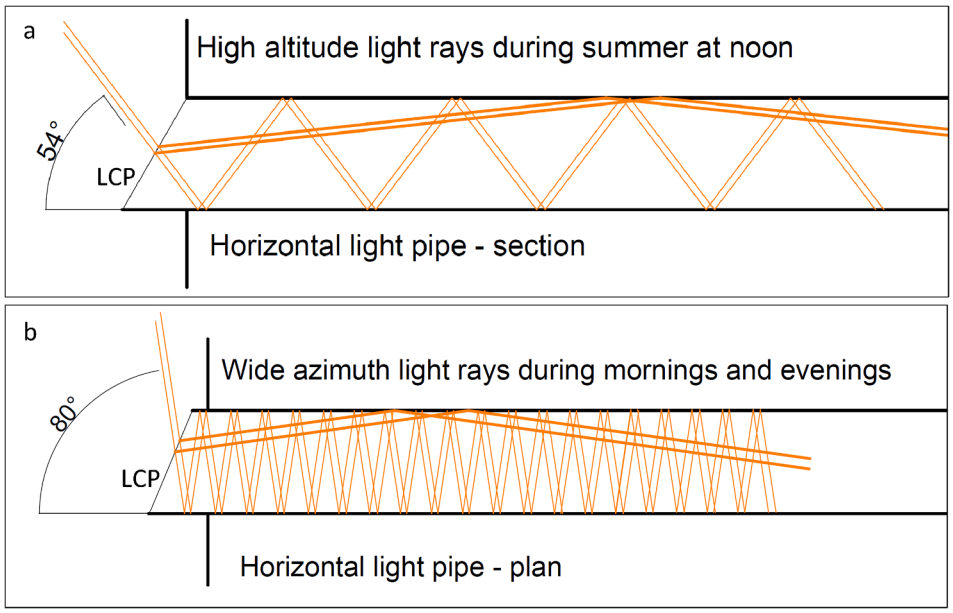

Fig. 2. The principle of LCP on the entrance of the horizontal pipe (adopted from (Garcia Hansen et al., 2001) (a) High-altitude light during summer at noon (section through the wall). Thicker line denotes deflected light that has preferable incident angle along the pipe's axis after deflecting on a tilted LCP; (b) wide azimuth light in the mornings and evenings (horizontal light pipe in plan). Thicker line denotes deflected light that has a preferable incident angle after deflecting on a single rotated LCP.

research, and the Conclusions chapter ends the study with the findings of the research. The paper is completed with Appendices A and B, which provide data on the experimental test applicable for further research, Appendix C, providing illustrations from the laboratory study, and Appendix D providing data on the uniformity of the direct light from the artificial sun at the Daylight laboratory at NTNU.

2. Methodology

The objective of the research is to determine how different LCP configurations (D/W, tilt, and rotating position) affect the light-pipe transmittance and to determine which configuration most improves the daylighting in the rear part of a typical office space. The assumptions of the study are that tilted LCPs with horizontal straight cuts will deflect the light from high-altitude angles and provide higher light transmission efficiency, while the two symmetrically rotated LCPs with vertical cuts will deflect wide azimuth, morning and evening light, and provide higher light transmission efficiency for unfavourable light incident angles. The assumptions are illustrated in Fig. 2a and 2b. Here, thin lines represent the usual light propagation in the pipe, and the thicker lines represent the light deflected through an LCP in front of the pipe. In order to see the effect of each LCP configuration during the entire year, the concept of daylight autonomy is applied for a certain work area inside the standard office space. The study is a pilot study for a full-scale experiment planned for an office building near Oslo (59°53′N, 10°31′E), Norway, which location determined the solar altitude and azimuth applied in the study.

The first part of the research comprises a parametric measurement of illuminance at the end of the tube under the several LCP configurations at the tube's entrance. The laboratory tests were done for direct illuminance using an artificial sun and for diffuse illuminance using an artificial overcast sky at Faculty of Architecture and Design (NTNU). The experiment was performed on a model of a horizontal light pipe with an aspect ratio (length-to-diameter) of p = 1200/150 mm (8). The study used four different LCP configurations (D/W), combined with three tilts and three rotations, for each testing solar altitude and azimuth position. The configurations (dimensions and tilt/rotation) of the LCP sheets used in this study are explained in Section 4.1, while the measuring procedure is explained in Section 4.2. The experiment was carried out in the summer of 2019.

To establish the adequate testing positions, the matrix of 15° azimuth and 5°/10° altitude (Table 1), was developed based on the solar chart for Oslo (Fig. 3). Due to the complexity and the size of the model, altitude 55° that corresponds best to highest altitude in Oslo (53°), could not be applied, instead the measurements were made with the altitude 50°.

After the measurements were taken, the transmittance efficiencies of the HPL of each LCP were calculated. The *CIE 173:2012 Tubular Daylight Guidance Systems* presented an approach to determine light transmittance efficacy called the "standard daylight guide characteristics" ***(η)*** (l'Eclairage, 2006). For each LCP configuration, the standard daylight guide characteristic ***η(T-R)***, was found from the ratio of the illuminance measured at the tubes exit, E*(T-R),* and the illuminance measured at the tube's entrance, E*(ZERO),* applying the calculation for each measuring position from the matrix (Eq. (5)).

$$\eta_{direct}(T-R) = E_{direct}(T-R)\tilde{A}\cdot E_{direct}E(ZERO) \quad (5)$$

Table 1
Testing matrix for parametric laboratory study that refers to the solar chart for a south facade in Oslo. Test points in colour represent typical analysing period of the year: red-summer, orange-late spring or early autumn, yellow-early spring or late autumn, blue-winter.

50°					50	50	50	50	50				
45°				45	45	45	45	45	45	45			
35°		35	35	35	35	35	35	35	35	35	35	35	
25°	25	25	25	25	25	25	25	25	25	25	25	25	25
15°		15	15	15	15	15	15	15	15	15	15	15	
5°		5	5	5	5				5	5	5	5	
Altitude/ Azimuth	90°	105°	120°	135°	150°	165°	180°	195°	210°	225°	240°	255°	270°
								not tested, assumed equal as the left side					

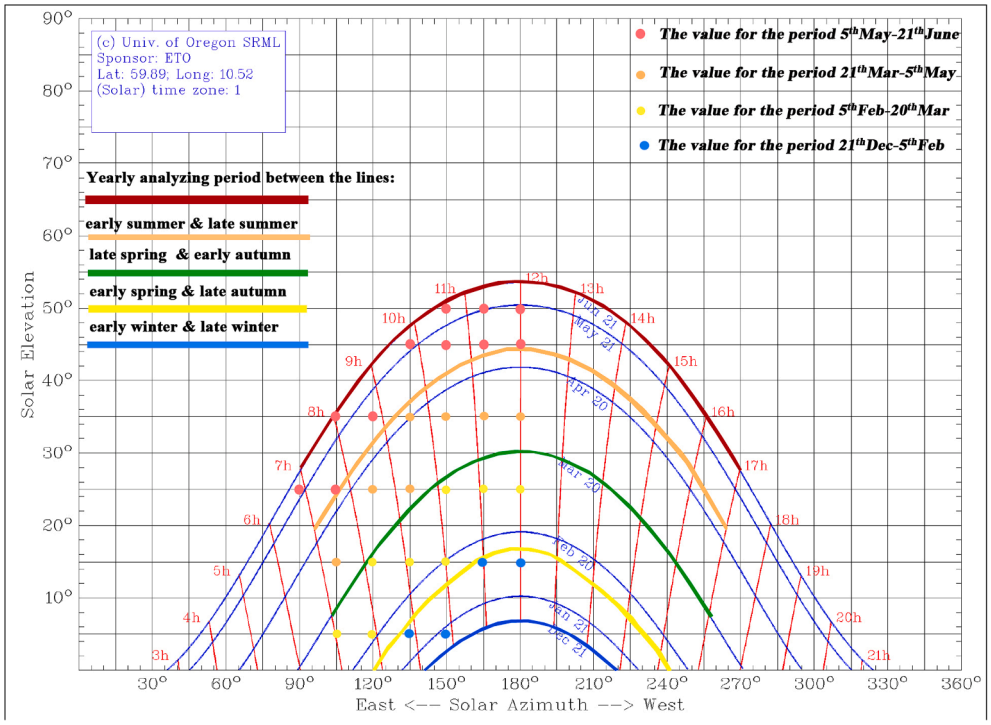

Fig. 3. Solar chart for Oslo (59°53′N, 10°31′E), Norway, with typical periods used in the analysis and testing position corresponding to the testing matrix retrieved from (SRML, 2019). Test points in colour represent typical analysing period of the year: red-summer, orange-late spring or early autumn, yellow-early spring or late spring, blue-winter.

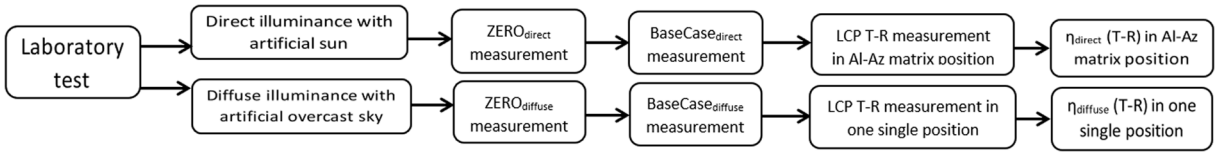

Fig. 4. Method of parametric study and determination of the standard daylight guide characteristic η(T-R).

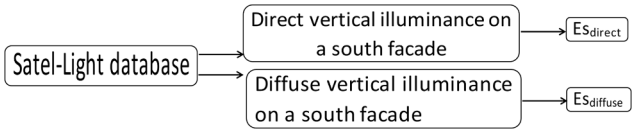

Fig. 5. Method for the development of Satel-Light data, $E_{Sdirect}$ and $E_{Sdiffuse}$.

A similar calculation was done for the diffuse illuminance as well, and Fig. 4 presents the method used in the laboratory study. The results for the standard daylight guide characteristic *η(T-R)* of the direct and diffuse illuminance are presented in Appendices A and B, respectfully. This data can be used to develop illuminance data for several other locations at latitudes ≥59° N because of the maximum tested solar altitude 50°) by using the Satel-Light data of direct vertical and diffuse vertical illuminance for the particular location.

The second part of the research is a daylight autonomy analysis of the daylight supplement through the horizontal pipe in the theoretical model of an office space. As the first part of the study resulted in a standard daylight guide characteristic ***η(T-R)*** for a pipe with an aspect ratio of 8, the absolute illuminance values from a Satel-light database are used in order to develop real illuminance values for the pipe's exit. Satel-Light data for the direct and diffuse illuminance on a vertical, south-oriented façade in Oslo was used (Fig. 5). Section 3 features the detailed procedure for the development of $E_{Sdirect}$ for a direct illuminance and $E_{Sdiffuse}$ for diffuse illuminance.

Real values for the illuminances at the tube's exit, Er_{direct} and $Er_{diffuse}$, were then developed by multiplying the standard daylight characteristic, ***η(T-R)***, with the absolute illuminance values from the Satel-Light database, Es_{direct} and $Es_{diffuse}$ (Eq. (6)). Eq. (6). is used for each LCP sample separately in each testing position from the matrix (Table 1).

$$Er_{direct}(T-R) = \eta_{direct}(T-R) \times Es_{direct} \quad (6)$$

The final Er_{total} is a result of the summation of Er_{direct} and $Er_{diffuse}$ for any testing configuration. Er_{total} is developed for the BaseCase (Eq. (7)) as well as for each LCP configuration (Eq. (8)).

$$Er_{total}(BaseCase) = Er_{direct}(BaseCase) + Er_{diffuse}(BaseCase) \quad (7)$$

$$Er_{total}(T-R) = Er_{direct}(T-R) + Er_{diffuse}(T-R) \quad (8)$$

Since the BaseCase test considered a completely open tube's entrance without any LCP and under the assumption that the entrance needs to be closed, the standard daylight guide characteristics (η) for the BaseCase were reduced by the standard light transmission factor for acryl (of 0.92).

In the theoretical model, the illuminance on the pipe's exit is directed down to the reference surface by a curved reflector. The theoretical model of the office space, the reflector, and the reference surfaces, together with the method for the calculation of illuminance on the reference surface, are explained in Section 5.

Table 2
Sunlight hours for Oslo (retrieved from Google, 2019).

Month	Jan	Feb	Mar	Apr	May	Jun	Jul	Aug	Sep	Oct	Nov	Dec	Annual
Average sunlight hours/day	01:27	02:56	04:54	06:04	07:30	08:08	07:03	05:54	04:36	02:48	01:22	00:48	04:28
Average daylight hours/day	06:50	09:05	11:46	14:35	17:09	18:40	17:58	15:38	12:51	10:03	07:29	06:02	12:00
Sunny/Cloudy daylight hours/day in %	22 /78	34 /66	43/57	43/57	45/55	44/56	40/60	39/61	37/63	29/71	19/81	14/86	37/63
Sun altitude at solar noon	10.3°	19.6°	30.4°	42°	50.3°	53.5°	50.5°	42.1°	30.7°	19.3°	10.1°	6.8°	30.5°

Table 3
Satel-light data for direct vertical illuminance Es_{direct} (in lux) on the south façade of an theoretical office building in Oslo (retrieved from Satel-Light (2019)).

50°					17,100	20,575	31,000	20,575	17,100				
45°				12,025	21,575	25,825	26,900	25,825	21,575	12,025			
35°		5650	8425	15,100	21,575	23,775	25,750	23,775	21,575	15,100	8425	5650	
25°	350	3600	8425	14,100	20,100	15,800	18,000	15,800	20,100	14,100	8425	3600	350
15°		2650	7675	5075	8450	11,275	13,100	11,275	8450	5075	7675	2650	
5°		700	1825	2500	3325				3325	2500	1825	700	
Altitude/Azimuth	**90°**	**105°**	**120°**	**135°**	**150°**	**165°**	**180°**	**195°**	**210°**	**225°**	**240°**	**255°**	**270°**

Table 4
Satel-light data for diffuse vertical illuminance, $Es_{diffuse}$ (in lux), on the south facade for Oslo (retrieved from Satel-Light (2019)).

50°					17,000	18,650	19,150	18,650	17,000				
45°				14,425	17,200	18,900	19,350	18,900	17,200	14,425			
35°		8625	10,850	14,225	17,200	13,525	15,025	13,525	17,200	14,225	10,850	8625	
25°	6000	7425	10,850	8225	11,350	8200	8800	8200	11,350	8225	10,850	7425	6000
15°		1750	4675	4075	6550	7300	7500	7300	6550	4075	4675	1750	
5°		200	400	1400	4250				4250	1400	400	200	
Altitude/Azimuth	**90°**	**105°**	**120°**	**135°**	**150°**	**165°**	**180°**	**195°**	**210°**	**225°**	**240°**	**255°**	**270°**

3. Outdoor daylight accessibility

The climate in Oslo is, in terms of the Köppen-Geiger classification, characterized by strong seasonality, snow, humidity, and warm summers (Dfb) (Kottek et al., 2006). According to historical weather recordings, there is a predominantly clear sky and sunlight for 37% daylight hours during the year, with the remaining 63% being predominantly overcast sky (Table 2).

It is generally assumed that the predominant type of sky in Norway is overcast, but the 37% of daylight hours throughout the year should not be neglected, as clear sky and sunlight represent the highest potential for light collection in any solar microclimate. Most of these sunlight hours occur during the summer half-year, when the sun's altitude and azimuth also have the biggest variation during the day. The cumulative sunlight hours for the summer half-year is 248 h, compared to 161 h for the winter half-year. The Satel-Light recordings (Satel-Light, 1998), based on the Meteosat Satellite images and obtained every half hour, are used to generate data on the direct and diffuse illuminance on a vertical south-oriented surface.

The direct and diffuse vertical illuminances from the Satel-Light were developed by following the data matrix in this study (Table 1) to correspond with the specific altitude and azimuth positions for each hour given by the Satel-Light data. Table 3 shows data for the direct illuminance and Table 4 shows data for the diffuse illuminance on the vertical south-oriented surface.

Illuminances on tilted surfaces (both vertical- and south-oriented in this study) are, according to the Satel-Light knowledge facts, computed from irradiances on tilted surfaces using the diffuse and direct luminous efficacies of the horizontal irradiance. The values obtained from the Satel-Light for each hour for a certain month are, developed as the monthly mean of hourly values.

A limitation of this study is that the direct and diffuse light from the Satel-Light database presents values from the real sky condition with an unknown distribution of luminance on the sky. This means that the values for direct and diffuse illuminances do not come from a static sun or sky with predictable light intensity and distribution, upon which the laboratory test in the present study was conceived.

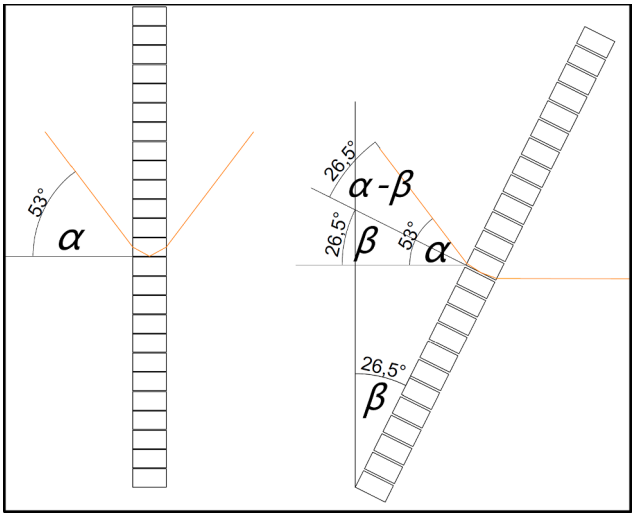

Fig. 6. Determination of real incident angle for the tilted LCP.

4. Experimental method for parametric measurements

4.1. Design basis

For the summer solstice in Oslo, Norway, the highest altitude of sun is 53.5° at 12:15 h (Fig. 3). At 7 AM, the altitude is close to 25° (at Az 90°), and at 5 PM, the altitude is close to 30° (at Az 270°). The spring and autumn equinoxes are characterized by solar altitude between 5° and 30° and azimuth between 95° and 255° for the usual user-occupancy period (7 AM–5 PM). For the winter solstice, the highest altitude is 6.8°, the lowest altitude 0° is at 09:30 h (Az is 140°), and the second-lowest altitude 0° is at 15:00 h (for Az 220°). The angles are rounded

Table 5
Solar altitude and azimuth during the summer solstice, equinox, and winter solstice during typical occupancy hours.

Season/solar altitude and azimuth	Altitude variation		Azimuth variations	
Time of the day	7 AM	12 AM	7 AM	5 PM
Summer solstice	25°	53°	90°	270°
Spring/autumn equinox	5°	30°	95°	255°
Winter solstice	0°	7°	140°	220°

4.1.1. Tilting LCP

For the light incident angle of 53.5°, and as can be seen in Fig. 1b, LCP D/W 0.3, tilted by $\beta = \alpha/2 = 26.75°$ will have almost 100% light deflection for the light incidence angle $\alpha = 26.75°$ relative to the LC panels. The angle through which the light would be deflected will be increased by the tilting angle of the LC panel *26.75°,* and the absolute outgoing angle will be 0° (deflecting angle 26.75°-tilting angle 26.75°)—relative to the pipes' s axis. The light will propagate an

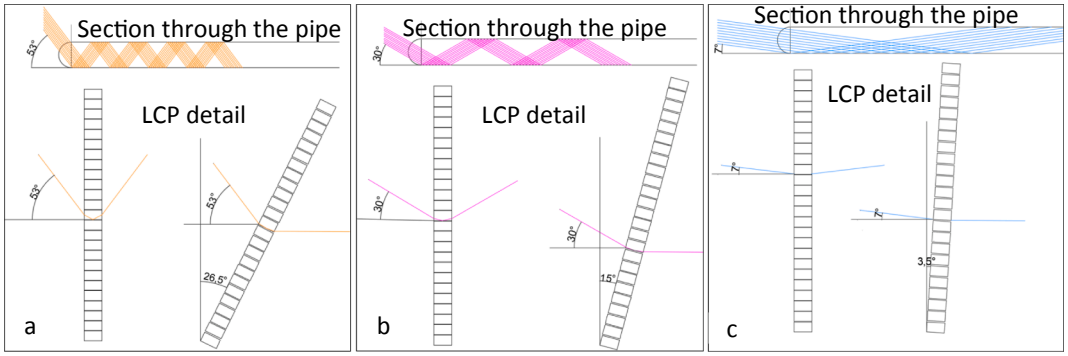

Fig. 7. The principle of light deflection for different altitude incident angles on a LCP with horizontal cuts; upper part of the illustration presents section through the horizontal pipe, and the lower part shows an enlarged section through the LC panel in the vertical and tilted positions; (a) Tilted LCP that deflects summer sunlight well at the highest altitude; (b) spring; and (c) winter.

to integers divisible by 5 for clarity.

The altitude variability is therefore 46.8° (53.5–6.8°), while the winter azimuth variability is 80° (for the first-lowest altitude 0°to the second-lowest 0°), and the summer azimuth variability is 180° (Fig. 3). This indicates that the variability in the azimuth angles should be the primary issue focused on in this study.

According to the light deflection theory of the LCP, if the aim is to have deflected light leaving the LCP and propagating along the pipe's axis, the LCP tilt/rotation should be $\beta = \alpha/2$, where α is a light incident angle on an LCP in the vertical position (Fig. 6.). In the case of the summer solstice, $\alpha_{max} = 53.5°$, the tilting angle is $\beta = 26.75°$. Table 5 presents the extreme altitude and azimuth incident angles for the Oslo location, which occur during the typical occupancy period (7 AM–5 PM). If the LCP is tilted by angle β, then α-β becomes a *real* incident angle for the tilted LCP (Fig. 6). In the case of strait cuts, $\theta = 0°$, as mentioned in the introduction, the *real* incident angle is α- $\beta = \alpha - \alpha/2 = \alpha/2$. The real incident angle α-β and the light deflecting factor (Fig. 1b) should determine the LCP's D/W configuration.

auxiliary within the tube without any interreflections, and the deflected light will be reduced just for the transmission factor of the acrylic panel (0.92).

For all incidence light falling between 53.5° and 26.75°, the fraction of deflected light will be reduced, and the fraction of directly transmitted light will be increased. For the incident light, exactly $\alpha = 26.75°$ light will be transmitted through the panel auxiliary at a transmission of 92%, while, for incidence light lower than 26.75° (October to February; Fig. 3), the light will be deflected through a much higher angle, which will increase the interreflections and reduce the light transmittance.

The principle of the tilting configuration that will best suit the light incidence angle during the summer solstice is presented in Fig. 7a along with that for the spring/autumn equinox in Fig. 7b and the winter solstice in Fig. 7c. See also Table 5 for altitude variations.

4.1.2. Rotating LCP

To manage the incident light with a non-preferable azimuthal angle, two symmetrically rotated LCPs with vertical cuts can be applied. They will deflect light rays with extreme azimuth angles and align them with

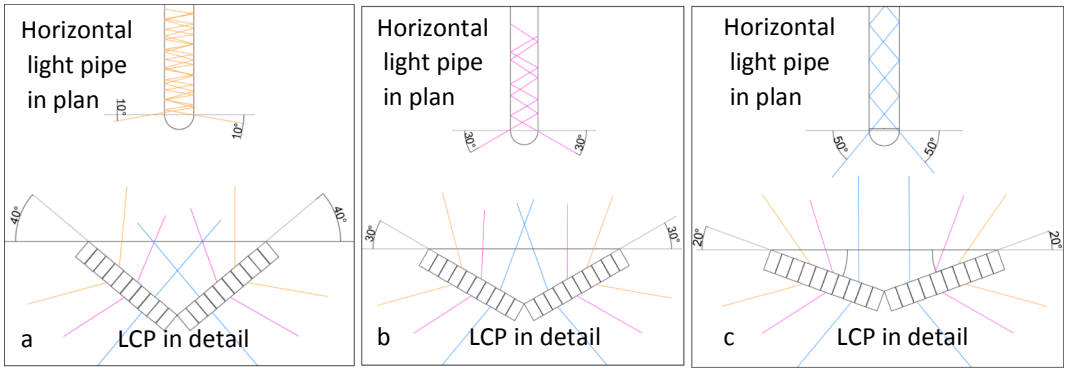

Fig. 8. The principle of light deflection for different azimuth incident angles on an LCP with vertical cuts; the upper part of illustration presents a plan through the horizontal pipe, and the lower part is an enlarged plan through two symmetrical LC panels in a rotated position; (a) LCP configuration that deflects summer sunlight well (orange rays); (b) LCP conf. that deflects spring sunlight well (pink rays); and (c) LCP conf. that deflects winter sunlight well (blue rays). (For interpretation of the references to colour in this figure legend, the reader is referred to the web version of this article.)

Table 6
LCP test configurations: D/W, tilting angles, and deflection factor for a certain light incident angle relative to the pipe's axis.

Testing configuration	D/W	Tilt	Deflection factor for an altitude incident angle relative to light pipe's axis		
ZERO	No LCP used – Sensors in the front of the tube	Measuring incident illuminance			
BaseCase	No LCP used – Sensors in the exit tube	Measuring output illuminance	34°	44°	54°
T-05-17	0.5	17°	0.50	0.65	0.88
T-05-22	0.5	22°	0.32	0.55	0.75
T-05-27	0.5	27°	0.20	0.45	0.65
T-06-17	0.6	17°	0.35	0.55	0.75
T-06-22	0.6	22°	0.25	0.45	0.65
T-06-27	0.6	27°	0.15	0.35	0.55

Table 7
LCP test configurations: D/W, rotating angles, and deflection factor for a certain light incident angle relative pipe's axis.

Testing configuration	D/W	Rotating angle	Deflection factor for an azimuth incident angle relative to light pipe's axis (0° azimuth is against north)		
Sample ZERO	No LCP used Sensors in the front of the tube	Measuring incident illuminance	90°/ 270°	100°/ 260°	110°/ 250°
BaseCase	No LCP used – Sensors in the exit tube	Measuring output illuminance			
R-08-20	0.8	20°	0.99	0.90	0.75
R-08-30	0.8	30°	0.90	0.75	0.60
R-08-40	0.8	40°	0.75	0.60	0.45
R-07-20	0.7	20°	0.85	0.99	0.85
R-07-30	0.7	30°	0.99	0.85	0.68
R-07-40	0.7	40°	0.85	0.68	0.50
R-06-20	0.6	20°	0.65	0.82	0.99
R-06-30	0.6	30°	0.82	0.99	0.80
R-06-40	0.6	40°	0.99	0.80	0.60
R-05-20	0.5	20°	0.40	0.58	0.80
R-05-30	0.5	30°	0.58	0.80	0.95
R-05-40	0.5	40°	0.80	0.95	0.70

the tube's axis (Fig. 2b). Since the azimuthal variability is symmetrical from the south-oriented pipe's point of view (east/west), the LCP should consist of two identical panels, each angled on its side (Fig. 8). In the case of the winter solstice sunrise, the altitude is 0° (at 09:30 h), and the Az is varying ±40° (Table 5), the LCP with vertical cuts should be angled $\beta = \alpha z/2 = 20^{\circ}$ in order to deflect the light auxiliary within the tube. In the case of the summer solstice, the solar azimuth ranges 90° to 270° from 7 AM to 5 PM. For $\alpha z = 90^{\circ}$, the LCP rotating angle should be $\beta = \alpha z/2 = 45^{\circ}$, and the real incident angle on an angled panel $\alpha z1 = \alpha z/2 = 45^{\circ}$. For the incidence angle of an $\alpha z1 = 45^{\circ}$, the LCP configuration of D/W 0.5 will provide the most effective deflection (Fig. 1b). For $\alpha z1 \leq 40^{\circ}$, the light will be deflected against the tube's walls, and the number of interreflections will increase, which will reduce the light transmittance.

The principle of the rotating configuration that will best suit the light incidence angle during the summer solstice is presented in Fig. 8a along with the spring/autumn equinox in Fig. 8b and the winter solstice in Fig. 8c.

4.1.3. LCP alternatives in the study

The proposed LCP configurations for variable altitudes and azimuth angles are presented in Tables 6 and 7. Due to the technical limitations of today's laser-cutting machines which cannot cut through acrylic plates thicker than 6 mm, the D/W varies between 0.5 and 0.8. Each LCP configuration has its biggest potential (highest deflection factor) for just a certain incident angle (Fig. 1b), and the other incident angles will result in reduced deflected and increased transmitted light. Tables 6 and 7 present the theoretical approach to the specific configuration. Each of the proposed configurations of D/W and the tilting/rotating angle is expected to balance the differences of the light pipe transmittance under the variable light incidence angle.

4.2. Experimental setup

In this experiment, an acrylic panel 6 mm in thickness (Plexiglas® XT 0A770, Evonik Performance Materials GmbH) was used for the LC panels. This acrylic panel is completely clear, transparent, and with a light transmittance of 0.92 and refraction index of 1.491.

The main issue in LCP fabrication, even nowadays, is that laser cutters are not designed to cut through acrylic panels thicker than 6 mm. The thickness of the plate dictates the distance-to-width ratio (D/W), and very narrow cut distances can bring about melting problems. Laser cuts were therefore done as D/W 0.5, 0.6, 0.7, and 0.8, which, for a panel 6 mm in thickness, gives distances of 3.0 mm, 3.6 mm, 4.2 mm, and 4.8 mm, respectively (Fig. 9).

During the design of the study, we considered a "climate envelope", which is necessary in real buildings to protect an indoor light pipe against the outdoor climate. The review of the commercial products on the market has shown that the most suitable and probable envelope shape would be a half-spherical dome (Fig. 10). The limitations in LCP configurations are the result of this assesment. The panels for the tilt probe were oval (d1 = 150 mm; d2 = d1/cos 45° = 212 mm), while, for the rotation probe, they were half-oval in shape (d1 = 150 mm; d2/2 = d1/2 * cos 45° = 106 mm). Fig. 10a and b illustrates the issue of the dome's shape limiting the tilt/rotation of the LCP. The tube was 150 mm in diameter and 1200 mm in length and was made of pap. The aspect ratio of the tube was L/D 1200/150 = 8. The tube was coated with

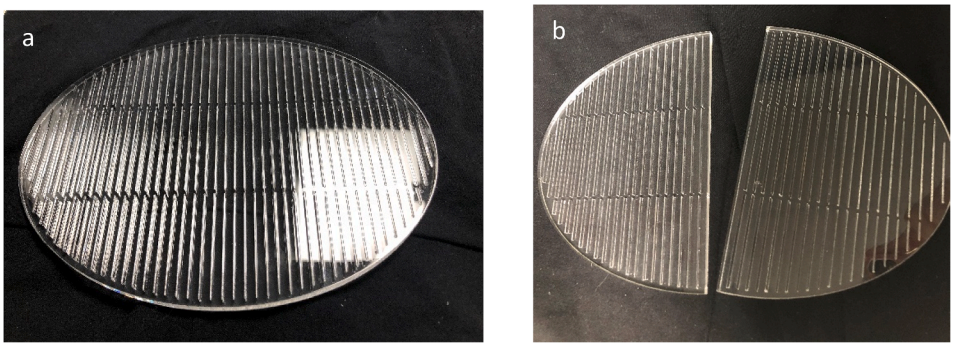

Fig. 9. (a) LCP in an oval shape for tilt probe; (b) LCP in half-oval shape for azimuth probe.

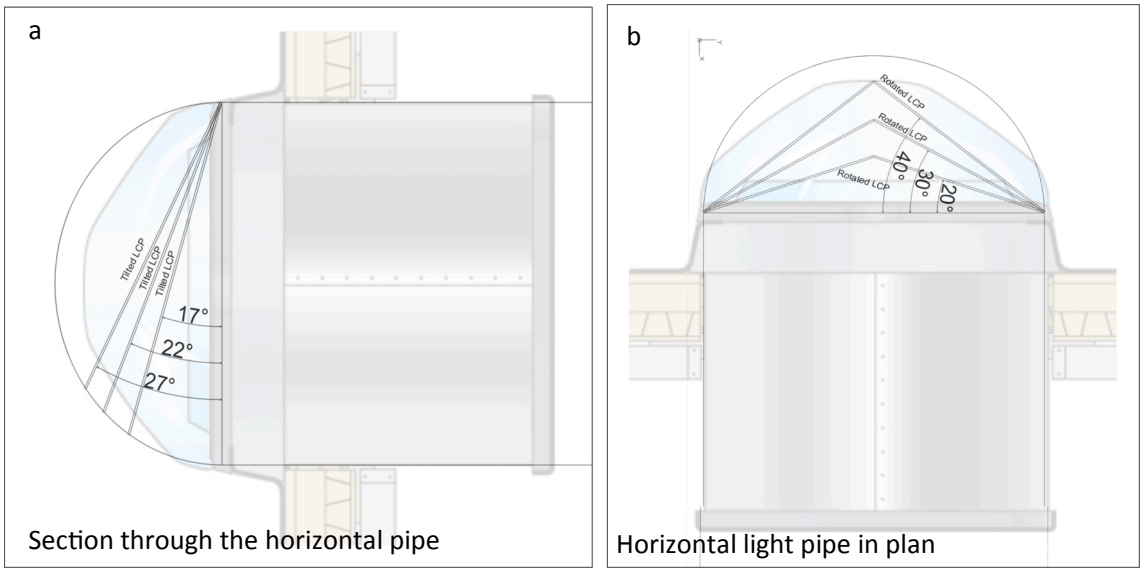

Fig. 10. (a) Tilt of LCP in an oval shape is limited by the shape of the dome; (b) rotation of symmetrically oriented LCP in half-oval shape is limited by height of the dome.

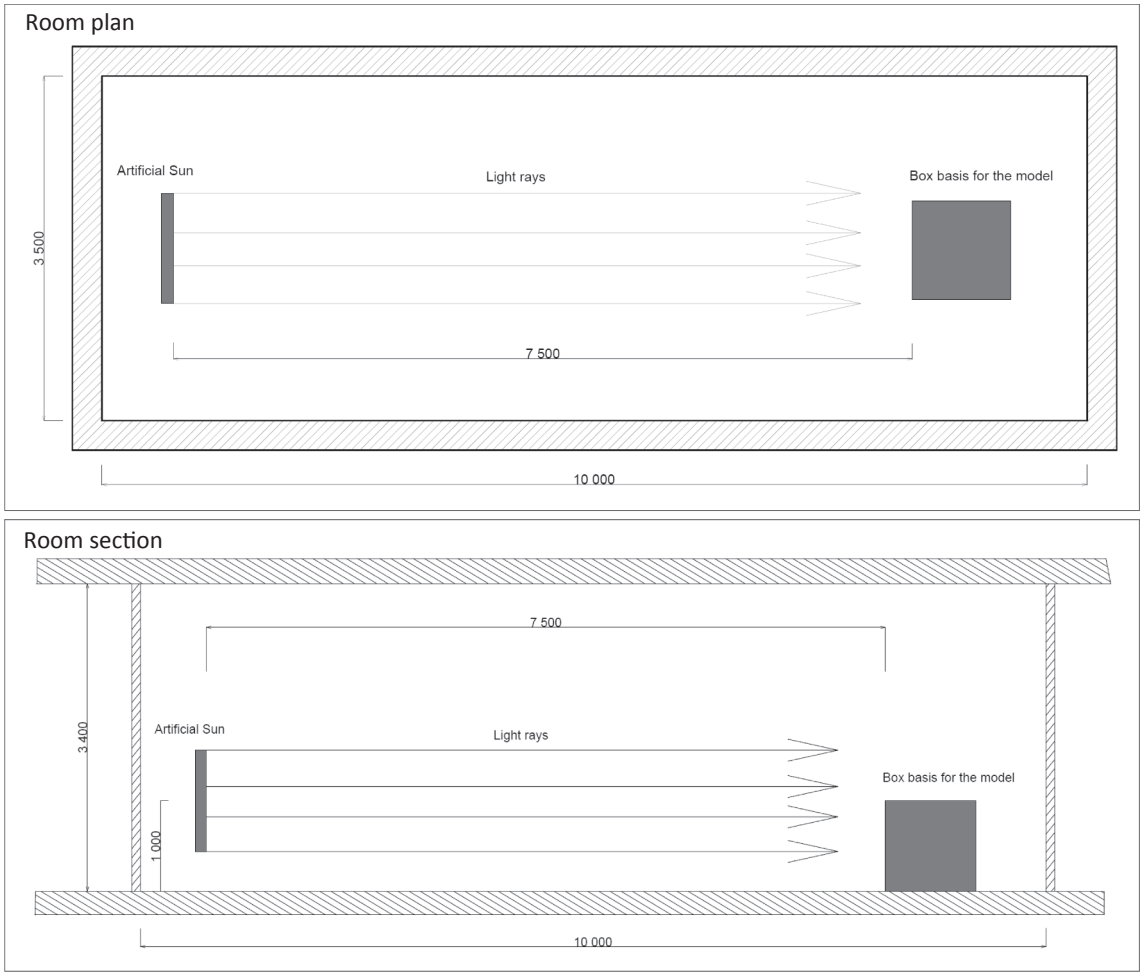

Fig. 11. Artificial sun setup in Daylight laboratory at NTNU, Faculty of Architecture and Design, in plan (up) and section (down).

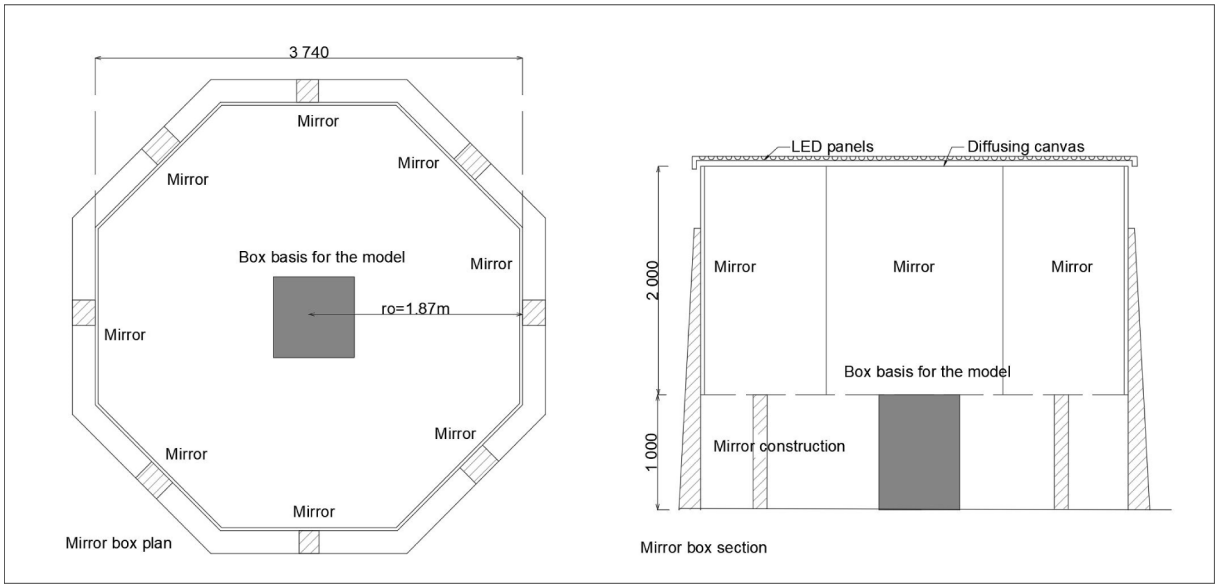

Fig. 12. Mirror box for artificial overcast sky study at NTNU, Faculty of Architecture and Design, in plan (left) and section (right).

specular mirror folium with 99% reflectivity (Specular silver film DF2000MA, 3M).

Lighting simulations were performed in the Daylight laboratory at NTNU, Department of Architecture and Technology. For the direct light test, an artificial sun was used, which was composed of 70 halogen lamps with parabolic reflectors (50 W) fixed to a vertical metal plate and arranged in a hexagonal pattern. The artificial sun provides close to parallel light beams with a dispersion angle of 3°. It was situated in a corridor-like room enabling long enought distance from the sun to the models, (Fig. 11). The walls, ceiling, and floor were painted matte black to minimize interreflections in the room and scatter light on the model. The model (tube) was positioned at the 7.5 m distance from the artificial sun, which ensured very even illumination. Actually, the uniformity of the light from the artificial sun on the tube's entrance, measured in the perpendicular direction to the sun, is 98%. The data is taken from the measurements done for the alternative ZERO for altitude 5° and azimuth 180°. The illuminance uniformity data for all matrix positions is presented in Appendix D.

The model was fixed on a box 1 m high so that the height of tube's entrance matched the centre of the artificial sun. For the altitude variation measurements, the model was tilted by lifting the back side on a vertical shelf, and azimuthal variation measurements were taken by rotating the box to align it with the angle grid on the floor. Testing positions were developed through the matrix of 5°, 15°, 25°, 35°, 45°, 50° for altitude, and 90°, 105°, 120°, 135°, 150°, 165°, 180° for azimuth (with the assumption that testing for azimuth 180–270° would be the same) (Table 1). The outermost azimuth angles, 90° and 270°, were taken from the vertical cut-off of the south façade and the user-occupancy hours, Table 5. Photos from the laboratory study are presented in Appendix C.

For the diffuse light experimental test, an artificial sky in the form of a mirror box at NTNU, Faculty of Architecture and Design, was used (Fig. 12). The mirror box was originally developed between 2000 and 2003 with fluorescent tubes and a translucent fabric suspended between the tubes and mirrors. In 2012, the tubes were replaced by RGBW LED chips, and the fabric by translucent acrylic ceiling plates. The box is designed octagonal in plan. This ensures more even light distribution horizontally when compared to rectangular mirror boxes that have slightly lower luminances in the vertical corners than the mirror centres. An octagonal box gives users more flexibility regarding the rotation of the model, as it does not matter whether the daylight opening in the model is oriented toward a mirror centre (Matusiak and Arnesen, 2005; Matusiak and Braczkowski, 2014). As the height of the tube's entrance is 150 mm, which is a 7.5% of sky height in the mirror box (2000 mm), it can be estimated that the parallax error is somewhat higher than 10% for low altitude angles (0–15°). For the altitude angles over 15°, as discussed in Lynes and Gilding (2000), the parallax error is lower than 10%. The test model was fixed on the table located in the middle of the mirror box. The height of the table was adjusted to align with the lowest edge of the mirrors. The tube was placed in one single position, with the opening at the centre of the mirror box based on the fact that the overcast sky simulated in the artificial sky chamber was rotationally symmetrical—that is, its luminance distribution was not dependent on the azimuth angle. Photos from the laboratory study are presented in Appendix C.

Lighting measurements were taken with five Almemo photosensors arranged in a cross on a circular surface, and the results were logged via Ahlborn logger and recorded via Almemo control software 6.0, Fig. C3, Appendix C.

5. Theoretical method for the daylight autonomy analysis

As mentioned in Section 3, the resulting Er_{total} represents the illuminance at the pipe's exit for each position from the matrix and each LCP configuration. In order to analyse the result of Er_{total} for the typical period, the concept of daylight autonomy (DA) in an imaginative working space was employed, assuming that illuminance on the working area was provided just through the horizontal light pipe. As discussed in the introduction, the daylight provision through the especially south oriented windows, are very much dependent on users' individual opinions about visual comfort, which most often results in closed blinds for much longer periods than strictly necessary, as users tend to instantly react based on discomfort, forgetting to open the blinds when the discomfort has passed. This results in unreliable daylight supplement inside—even for working places closest to the window.

According to *EN17037:2018 Daylight in Buildings*, the recommendation for the "minimum level" target illuminance of 300 lx for 50% of reference surface area and 100 lx for 95% of a reference surface area; for the "medium level", a target illuminance of 500 lx for a 50% of reference surface and 300 lx for a 95% of reference surface; and, for a "high level", a target illuminance of 750 lx for a 50% of reference surface and 500 lx for a 95% of reference surface has to be fulfilled for a 50% of daylight hours. Following those recommendations (noting that the requirements for 50% of working surface in a room with window(s) in one wall is

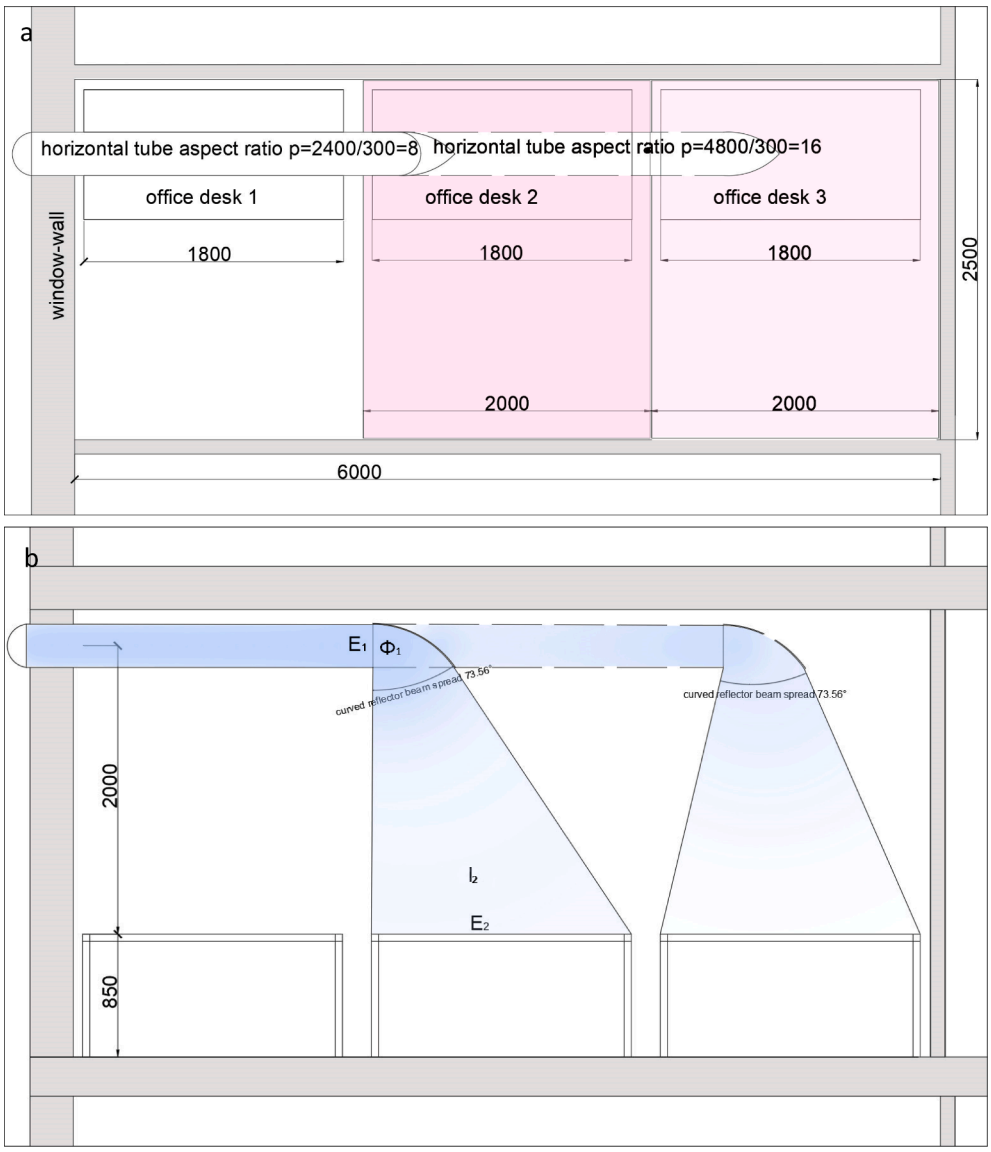

Fig. 13. (a) Plan and (b) vertical section of a typical office (the second and third working areas in the office, correspond to a light pipe of aspect ratio 8 and 16, respectively).

relevant only for the window zone), both a minimum level (DA_{100} for 95% of a ref. surface) and medium level (DA_{300} for a 95% of a ref. surface) are considered for a reference surface 0,85 m above the floor.

The straight horizontal tube, of aspect ratios 8 and 16, is considered in the theoretical model of the office space. The tube of the aspect ratio 8 has a length of 2.4 m and a diameter of 30 cm, while the tube of aspect ratio 16 has a length of 4,8m and a diameter of 30 cm. Assuming a wall thickness of 30 cm, the tube's exit is 2.1 m from the wall inside in the first theoretical case and 4,5 m in the second, which corresponds to the second and third working area from the window (Fig. 13). For the tube with an aspect ratio 8, the Er_{total} from the laboratory parametric study was used. For the tube with an aspect ratio 16, the tube transmission efficacy factor (TTE) described in CIE 173:2006 was used to estimate the transmission reduction on the basis of the increased length of the pipe (l'Eclairage, 2006). The approach of TTE was developed for vertical light pipes under an overcast sky, assuming that only light within a cone subtending an angle of 30° enters the tube. Under the circumstance of lacking a simple method for tube transmission efficacy estimation under other sky conditions, as well as a wider range of light incident angles, the TTE approach can be applied under the clear notice of an approximation. According to Table 2 (l'Eclairage, 2006), for a pipe reflectance at a min. of 0.995 and an aspect ratio of 8, the TTE is 0.97, and, for the aspect ratio of 16, it is 0.93. As the Er_{total} for the aspect ratio of 8 is already known (and is strongly dependent on LCP configurations), the Er_{total} for the aspect ratio of 16 will be calculated from the value of Er_{total} for the aspect ratio of 8 by reducing it for the difference factor of $TTE_{16}/TTE_8 = 0.93/0.97 = 0.958$.

It is considered that a certain portion of the light leaving the pipe is diffused and cannot be perfectly directed to the desired area (in this case, to a curved reflector explained further in the text). To account for this, the resulting illuminances on the pipe's exit, $Er_{total,}$ is reduced by 10%. The mounting height of the tube above the workplane is d = 2 m (Fig. 13). It is assumed that the daylight on the exit of the tube is reflected by the curved reflector of a high light reflectivity (99%), which features a beam spread covering the area corresponding to the reference surface $A = 5\ m^2$, as it is supposed to be round. The solid angle (Ω) of the reflector is, in this case, 1,25 Sr (Eq. (9)). The beam spread of the reflector is $\delta = 73.56°$ (Eq. (10)).

$$\Omega = A \div d^2 \tag{9}$$

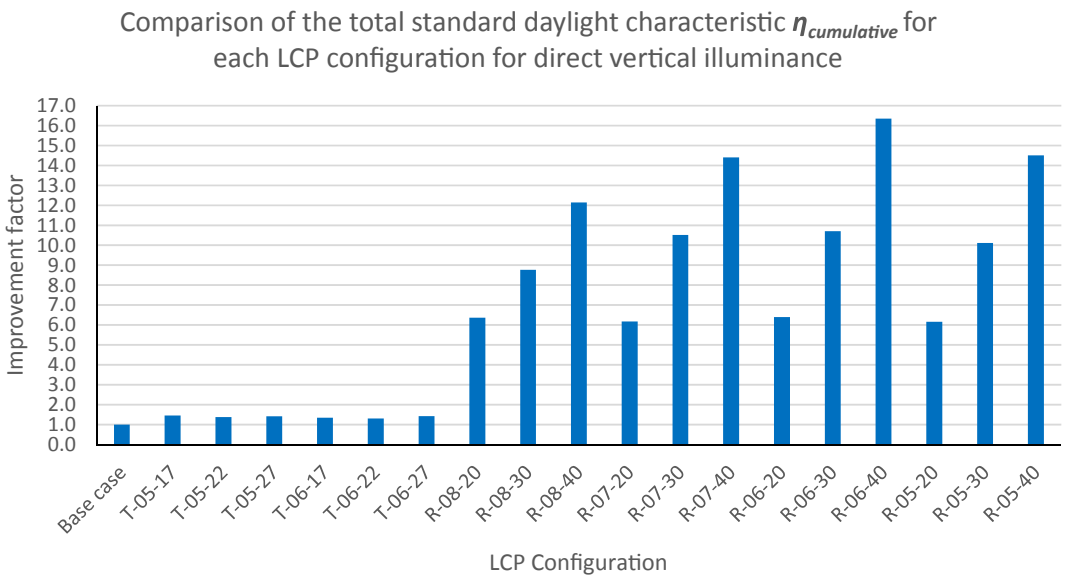

Fig. 14. Comparison of the standard daylight characteristic $\eta_{cumulative}$ for each LCP conf. for direct vertical illuminance (aspect ratio 8).

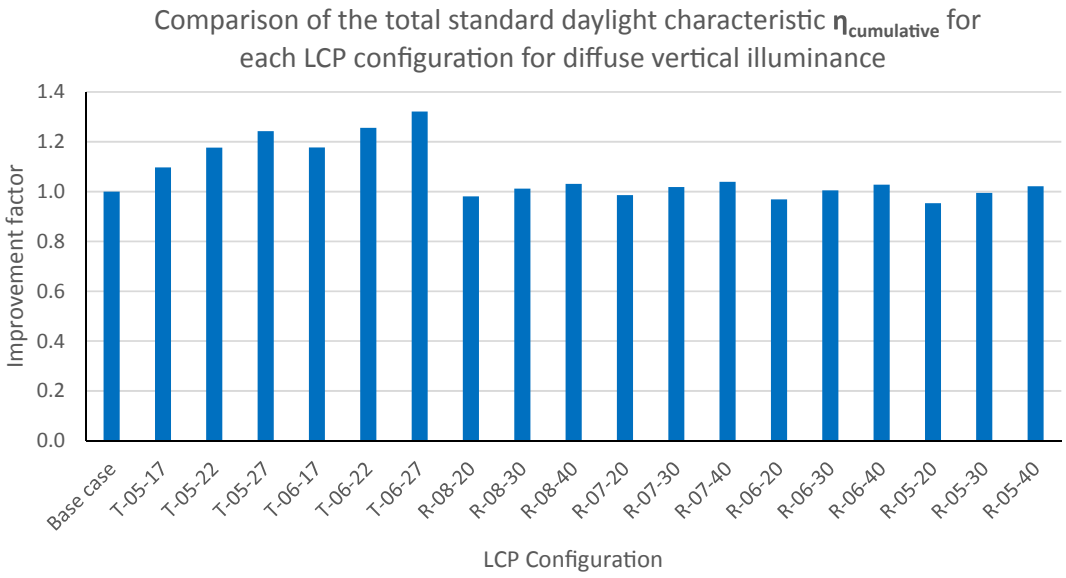

Fig. 15. Comparison of the standard daylight characteristic $\eta_{cumulative}$ for each LCP conf. for diffuse vertical illuminance (aspect ratio 8).

$$\Omega = 2\pi\left(1-\cos\frac{\delta}{2}\right) \tag{10}$$

$$I_2 = E_2 \times d^2 \tag{11}$$

$$\Phi_1 = \frac{I_2}{0.9 \times \Omega} \tag{12}$$

If a threshold illuminance on the reference surface is E_2 (in this case, 100 lx and 300 lx), the threshold light intensity, I_2, is 400 cd and 1200 cd, respectively (Eq (11)). However the inverse square low (Eq (11)) can be used just for point sources where largest dimension of the source (here tube's exit) is not less than one fifth of the distance to the reference surface. The required light flux from the curved reflector, Φ_1, is dependent on the light beam spread but also the portion of light inevitably scattered outside the beam spread of the reflector and against the walls. It can be taken that this portion, for a room with light walls (reflectance > 70%) reflecting most of the diffuse light back to the reference surface is 10%. The required light flux, Φ_1, can be derived from Eq. (12). In order to have a threshold value in lux to could compare with the results from the parametric study, E_1, is derived from Eqs. (13) and (14). The tube diameter (D_p) is 30 cm, and its exit surface (P_t) is 0.071 m^2. The required E_1-threshold value of DA_{100} is 7746 lx, and that of DA_{300} is 23,239 lx.

$$P_t = \pi \times D_p{}^2 \tag{13}$$

$$E_1 = \frac{\Phi_1}{P_t} \tag{14}$$

The threshold values E_1 for DA_{100} and DA_{300} are used to determine the number of hours in the resulting Er_{total} for each LCP configuration. In the position matrix, typical analysing periods are determined from the position of the sun's altitude and azimuth. The typical analysing periods are winter, early spring/late autumn, late spring/early autumn, and summer. It can be noted from Fig. 3 that the depicted periods, with their characteristic Al and Az, will occur two times throughout one entire year.

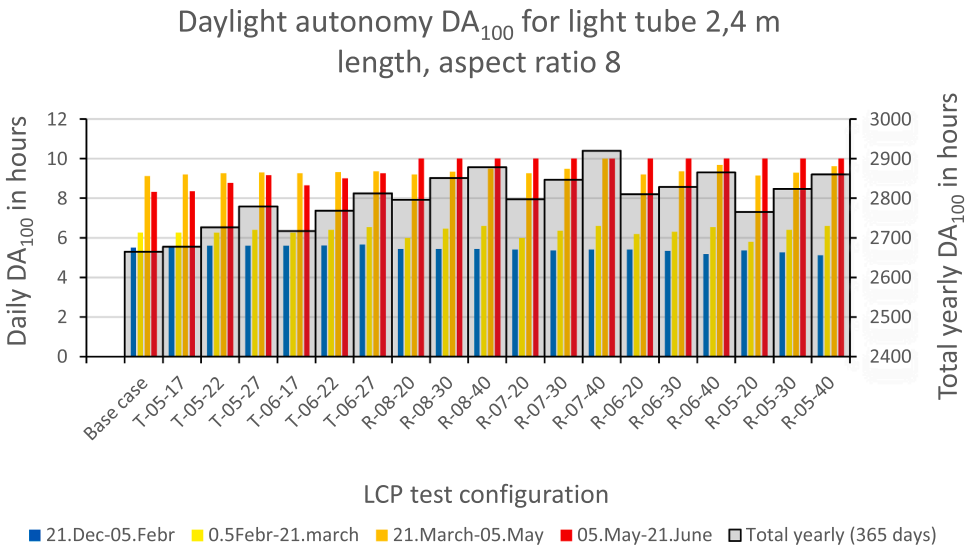

Fig. 16. DA in hours for each LCP configuration when illuminance exceeds 100 lx on the reference surface, aspect ratio 8.

6. Results

The results for the standard daylight guide characteristic *η(T-R)* (for direct and diffuse illuminance) for each LCP configuration and in each testing matrix position are presented in Appendices A and B.

In order to compare the standard daylight guide characteristic, – *η*, for each LCP configuration with the BaseCase, $\eta_{cumulative}$, (where *η* for a certain LCP configuration is aggregated) is presented in Figs. 14 and 15 for direct and diffuse illuminance, respectively. The presented ***η(T-R)*** refers to the tube with aspect ratio of 8.

The standard daylight guide characteristic (***η***) for all R-LCP configurations increased from 6 to over 16 times for direct light when compared with the BaseCase (Fig. 14). The T LCP configurations show a slightly increased ***η***, with 1.46 times (46%). Fig. 15 shows that the highest increase in ***η*** for diffuse light occurs in T LCP configurations— in fact, up to 1.32 times (32%), while none of the R LCP configurations show any significant increase. The very high increase in η for the R samples can be explained through the difference between the extreme incident angles, which are, in the case of altitude variability, 46° and, in the case of azimuth angles, up 2 × 90°. Some of the LCP configurations also have a very high deflection factor for some of the extreme azimuth angles (see Tables 6 and 7).

The final Er_{total}, as a result of the summation of Er_{direct} and $Er_{diffuse}$ for any testing configuration, was used to check if the threshold value (E_1) was achieved. The values are not presented in this study due to their non-universality, as they are only applicable to the Oslo-solar microclimate, but they are available upon request.

The results of DA_{100} and DA_{300} for a theoretical model of an office space with tube aspect ratios of 8 and 16 are analysed. The DA in this project is presented in hours (instead of a percentage of daytime) simply because this study addresses a typical office building with strictly defined occupancy time, that is from 7 AM to 5 PM. The time before and after is just not relevant.

The total yearly DA in hours can be calculated by multiplying daily DA of each period by the number of days in that period. As mentioned in the introduction, the solar position will take place twice during each analysing period throughout the year. There are 4 typical periods, and the number of days in each period is ¼ of the 365 days or 91.25 days. The total yearly daylight autonomy in hours is: $DA_T = VinterDA_d * 91.25 + EarlySpringDA_d * 91.25 + LateSpringDA_d * 91.25 + SummerDA_d * 91.25$.

Starting the analyses, the first issue to check was whether any of the

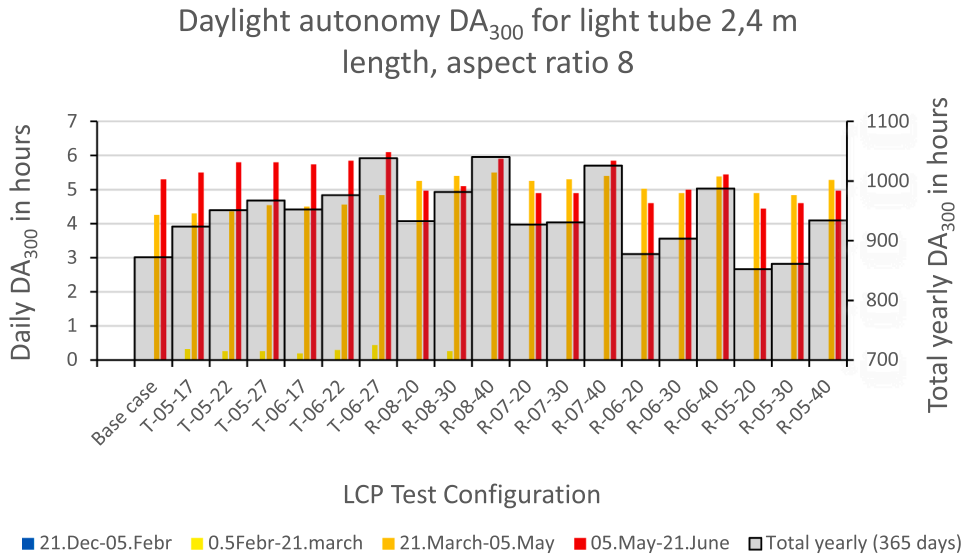

Fig. 17. DA in hours for each LCP configuration when illuminance exceeds 300 lx on the reference surface, aspect ratio 8.

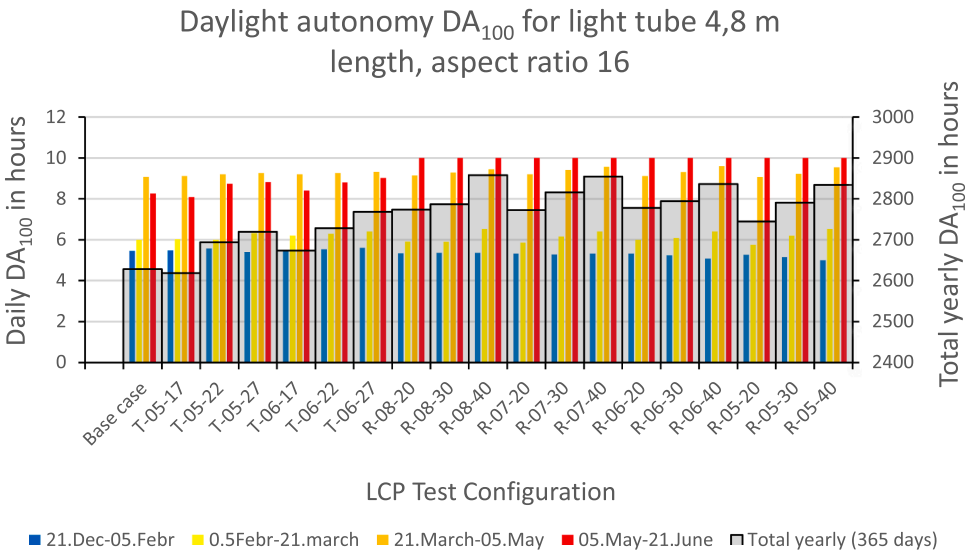

Fig. 18. DA in hours for each LCP configuration when illuminance exceeds 100 lx on the reference surface, aspect ratio 16.

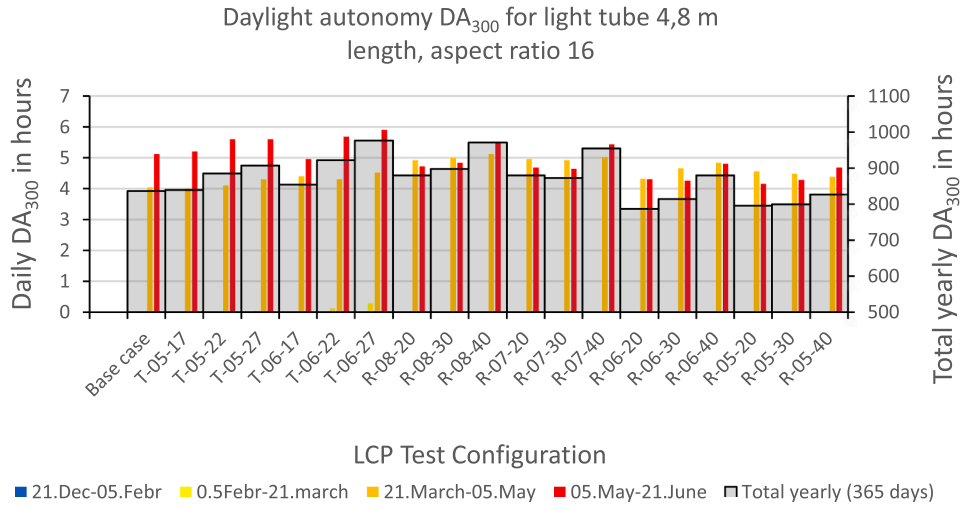

Fig. 19. DA in hours for each LCP configuration when illuminance exceeds 300 lx on the reference surface, aspect ratio 16.

LCP configurations decreased the DA when compared to the BaseCase. The values show that none of the LCP configuration decreased the DA_{100}, while the decrease was present for several R LCP configurations for DA_{300}. This is noticeable for both aspect ratios of 8 and 16.

The analysis of DA_{100} for the aspect ratio of 8 (Fig. 16) shows that the R-LCP configuration with a 40° rotation produces the highest improvement in total yearly DA hours by up to 10% for R-07-40. The improvement is mostly noticeable during the summer months, where, each day, the DA is prolonged by nearly two hours.

The analysis of the DA_{300} for the aspect ratio of 8 (Fig. 17) shows that the increase in terms of the total yearly hours is highest for T-06-27, R-08-40, and R-07-40 of up to 19% longer yearly DA in hours. The highest improvement happens during the late spring, with 1 h and 20 min each day. It can be noted that all T configurations prolonged DA_{300} during the early spring up to 30 min in the case of T-06-27, while none of the R configurations showed improvements. The reduction in daily hours during the summer is also noticeable for configurations R-05-40, R-05-30 and R-06-40 and R-06-30, while they contribute to the DA positively during the late spring. This can be explained by total movement of light incident angle throughout the day, which in case of spring is not as wide as in case of summer, and the LCP R configurations that are rather successful in light transmission of the spring light rays than light deflection of the summer light rays.

The results for the tube with an aspect ratio of 16 show a similar tendency (Figs. 18 and 19). For DA_{100}, it is possible to expect 10 h of daylight supplement during the summer using any of the rotated LCP configurations, which is one hour and 45 min longer than in the BaseCase. The total yearly improvement is most noticeable in the R-08-40 and R-07-40 configurations, with up to 8.75% each. For DA_{300}, the highest improvement in total yearly hours is noticeable for T-06-27, R-08-40, and R-07-40, with up to 16%. Meanwhile, T-06-27 especially enables longer visible DA_{300} during the early spring. A reduction similar to that with the aspect ratio of 8 is noticeable for configurations R-05-40, R-05-30, R-06-40, and R-06-30, to which they contribute during the late spring but prevent during the summer.

An analysis of the total yearly DA hours between a light pipe with an aspect ratio 8 versus 16 shows that there is a reduction in the number of hours for about 6%. This information can be useful for a simple estimation of DA for pipes even longer than 4.8 m. The daily DA_{100} in hours still shows the possibility of 10 h of 100 lx at a 4.5 m distance from the façade wall during the summer period. DA_{300} will be achieved for almost six hours during the same period. The total yearly DA_{300} for LCP configuration T-06-27 shows that the daylight requirements of the working place 4.5 m from the façade are fulfilled for 976 h.

Tilted-LCP configurations should deflect high-altitude light well, which can take place during the summer at noon. This effect is

noticeable in the results of Er, but, since all the LCP configurations give equal DA for the number of hours during the summer, the improvement is not as distinguishable as during the winter period. In the winter period, the portion of the diffuse light is much higher (in total) than the portion of the direct light; the fact that illuminance (either diffuse light in artificial sky or diffuse light from the Satel-Light) is increasing with altitude is reflected in the results.

The rotating LCP configurations give no indication of improvement during the winter, which was expected, and they also show a decrease during the early spring when compared with the BaseCase. An increase in DA hours for the R LCP is noticeable during the late spring and summer, which are associated with wide azimuth incident angles, but it appears that the D/W of the LCP is steering the potential.

Even the base base of the horizontal light pipe without any LCP on the entrance enables a minimum of five hours of 300 lx illuminance for both the 8 and 16 aspect ratios. The aspect ratio of 16 especially corresponds to the area where a window does not provide enough daylighting and electrical lighting needs to be used during all occupancy hours.

7. Discussion

User-controlled sun-shading devices are often the cause of a radical reduction in daylight availability during the day, with daylight contribution through the window then being very much dependent on the weather conditions and single-user behaviour. In general, users react instantly based on discomfort (glare or overheating) by closing sun-shading devices and are not that eager to open them again, which results in a much lower use of daylight than is theoretically possible. Automatically controlled sun-shading devices cause large and unpredictable changes in the luminous environment via switching between light and darkness. This paper shows that using a horizontal light pipe with a LCP can increase daylight autonomy in the indoor space of an office building and improve the reliability of daylight. More reliable daylighting in the indoor space will increase visual comfort and user satisfaction. In the mornings, daylight levels could be higher compared to a room with a side window. The highest improvement can be noted in the summer, and with the coincidence of the glare and thermal-load occurrence. The benefit of supplying the inner space with natural lighting becomes even more significant during the time when daylighting is drastically reduced by sunscreens.

It was discovered through the T and R LCP configurations tests that almost all T configurations work well with an overcast sky and R LCP configurations work well with sunlight. This fact could be used to design LCP configurations for north-oriented horizontal tubes. The portion of diffuse light on the north-oriented façade is undoubtedly higher in comparison to direct light, but direct light does still occur in the early mornings and evenings during the summer (Oslo, 59°N). Direct light on the north façade can appear when it is not needed (for commercial functions), but it can be quite appreciated during nightshift activity in industrial buildings. The T LCP configurations that show the highest improvements in diffuse light transmittance through the tube, (η), could be used to improve the performance of horizontal daylight tubes on the north facade. For the east and west oriented facades, a combination of tilted (T) LCPs against the north and rotated (R) LCPs against the south could be a successful solution, but this needs to be further tested.

By applying one single fixed solution, the full theoretical potential of LCP configurations cannot be utilized, but the possibility of the passive (user-operated) steering of the LC panel by rotating it along the tube's circumference could lead to greater DA improvements than that presented in this study. A season-dependent adjustment could be also applied.

As daylighting through the side window drastically decreases with distance from the facade, the extremely uneven lighting level affects the threshold sensitivity of the light controlling system and the possibility of reducing artificial lighting to conserve energy. This paper shows how the daylight level deeper in the space can be increased and produce balance across the entire room, which will also give more reliable data to light sensors and ensure lower energy use. The study demonstrates an improvement of 10% for DA_{100} and 19% for DA_{300} for the aspect ratio of 8, while 8.75% for DA_{100} and 16% for DA_{300} for the aspect ratio of 16 are shown on a yearly basis when compared to the BaseCase.

Limitations of the experiment included the following: the LCP samples were not perfectly cut due to the laser-cutter technology resulting in cuts with a chamfer on the LCP's frontside. There was also a possibility that some of the measurements had systematic errors caused by the manual handling of the model and LCP samples.

Also, a diffuse luminance distribution under the real sky, which depends on sun position and cloudiness, is different from the luminance distribution of diffuse light under an artificial sky at the Daylight laboratory at NTNU, which is a static simulator of a standard CIE overcast sky with a 1:3 luminance ratio (horizon:zenith) and rotational symmetry. To combine the standard daylight guide characteristics (η) for diffuse light measured under the artificial sky with diffuse illuminance from Satel-Light is a simplification. Still, we posit that this simplification can be defended because it gives conservative rather than overoptimistic DA results. The CIE model of the overcast sky represents the worst case of luminance distribution compared to the blue sky with sun, which features a very bright area around the sun (called the corona). The light from the corona, which is included in the diffuse illuminance from Satel-Light, will behave quite similarly to the light from the sun, because the incidence angle of light from corona is close to the incidence angle of the light from the sun. The scenarios that function well with the direct light from sunlight will perform even better than presented in this study due to the additional contribution from the corona if the sky is clear around the sun (compared to the CIE-overcast sky). This means that improvements due to the diffuse light will be higher for the clear sky with sun than for the CIE overcast sky in the best scenarios.

8. Conclusion

This paper shows how the illuminance levels inside the room at a 2.1m and 4.5m distance from the façade can be increased by daylight being transported through a horizontal light pipe equipped with a static light deflecting panel, LCP, at the pipe's entrance. Two types of the LCPs were considered, T – tilted with horizontal cuts and R – rotated with vertical cuts

The study shows that a horizontal light pipe, even without any LCP on the entrance, makes a significant positive contribution to daylighting, and that T LCPs work best under an overcast sky and R LCPs work well with sunlight.

Tilted LCPs with horizontal cuts effectively deflect light of higher altitudes and increase light transmittance (η) of the tube, but this is mostly significant during the winter, when most of the light is diffuse. In the buildings where winter daylighting is highly appreciated for health and wellbeing, as in healthcare facilities or in schools, the tilted LCPs with horizontal cuts could be a very valuable application.

During the summer, the light flux transported through the tube equipped with tilted LCPs was significantly higher than the minimum required illuminance at the tube exit, which indicates that the light could be conveyed at a longer distance.

Two symmetrically rotated LCPs with vertical cuts increase the light transmittance (η) of the tube for morning and evening light especially during the summer. As such, they could be even more attractive for buildings used also during evening. R LCPs showed no improvement in DA_{100} or DA_{300} during the winter.

The analysis of total yearly DA hours with minimum 100 lx (DA_{100}) shows similar results for both aspect ratios (8 and 16). The R-LCP configuration with a 40° rotation makes the highest improvement (up to 10% for aspect ratio 8). The improvement is mostly noticeable during the summer months, where the DA is prolonged by nearly two hours a day.

The analysis of the total yearly DA hours with minimum 300 lx (DA_{300}) for both aspect ratios shows that an increase of up to 19% is possible. The highest improvement (1 h and 20 min a day for the 8 aspect ratio) happens during the late spring.

Declaration of Competing Interest

The authors declare that they have no known competing financial interests or personal relationships that could have appeared to influence the work reported in this paper.

Acknowledgements

This study was conducted as a part of a PhD-study at the Norwegian University of Science and Technology with the support of Norconsult AS and the Norwegian Research Council.

Contributions

B.O. conceived and wrote the study; B.M. helped define the scope of the study and the methodology, gave feedback on the content of the paper, and contributed by performing quality assurance and proofreading.

Appendix A. Standard daylight characteristic of LCP configuration for the direct vertical illuminance *ηdirect(T-R) = Edirect(T-R)/Edirect(ZERO)*

See Tables A1–A19.

Table A1
η BaseCase.

50	0	0	0	0	0.68	0.83	0.85						
45	0	0	0.70	0.76	0.91	0.90	0.81						
35	0	0.35	0.84	1.00	0.85	0.87	0.83						
25	0.15	0.62	0.79	0.75	0.76	0.82	0.91						
15	0.36	0.61	0.74	1.07	0.96	0.94	0.87						
5	0.87	0.94	1.14	1.07	0.76	0.79	0.91						
	90	105	120	135	150	165	180	195	210	225	240	255	270

Table A2
η T-05-17.

50	0	0	0	0	0.75	0.83	0.93						
45	0	0	0.90	0.79	0.84	0.8	0.89						
35	0	0.53	0.76	0.87	0.78	0.89	0.88						
25	2.19	0.61	0.74	0.70	0.77	0.76	0.88						
15	2.44	0.66	0.68	0.96	0.88	0.89	0.82						
5	7.76	0.72	0.81	0.99	0.68	0.76	0.88						
	90	105	120	135	150	165	180	195	210	225	240	255	270

Table A3
η T-05-22.

50	0	0	0	0	0.76	0.87	0.96						
45	0	0	0.88	0.87	0.83	0.78	0.89						
35	0	0.56	0.78	0.88	0.79	0.89	0.87						
25	1.70	0.67	0.76	0.71	0.76	0.76	0.80						
15	2.45	0.69	0.69	0.88	0.86	0.85	0.79						
5	6.81	0.75	0.80	0.96	0.66	0.74	0.82						
	90	105	120	135	150	165	180	195	210	225	240	255	270

Table A4
η T-05-27.

50	0	0	0	0	0.73	0.88	1.00						
45	0	0	0.76	0.82	0.9	0.87	0.96						
35	0	0.52	0.74	0.87	0.79	0.84	0.9						
25	2.13	0.67	0.78	0.72	0.75	0.74	0.76						
15	2.24	0.72	0.71	0.93	0.85	0.81	0.76						
5	6.49	0.79	0.81	0.95	0.64	0.70	0.76						
	90	105	120	135	150	165	180	195	210	225	240	255	270

Table A5
η T-06-17.

50	0	0	0	0	0.77	0.9	0.97						
45	0	0	0.87	0.90	0.86	0.98	0.93						
35	0	0.57	0.80	0.89	0.79	0.88	0.87						
25	1.94	0.6	0.75	0.72	0.76	0.75	0.74						
15	1.97	0.64	0.68	0.96	0.91	0.82	0.84						
5	5.97	0.70	0.81	0.99	0.69	0.78	0.86						
	90	105	120	135	150	165	180	195	210	225	240	255	270

Table A6
η T-06-22.

50	0	0	0	0	0.77	0.85	1.0						
45	0	0	0.8	0.78	0.89	0.87	0.9						
35	0	0.55	0.76	0.87	0.77	0.87	0.87						
25	1.59	0.64	0.77	0.73	0.78	0.77	0.72						
15	1.88	0.68	0.68	0.95	0.9	0.79	0.8						
5	5.63	0.74	0.82	0.96	0.66	0.74	0.81						
	90	105	120	135	150	165	180	195	210	225	240	255	270

Table A7
η T-06-27.

50	0	0	0	0	0.77	0.89	0.95						
45	0	0	0.93	0.85	0.89	0.87	0.9						
35	0	0.8	0.76	0.87	0.77	0.88	0.83						
25	1.91	0.64	0.77	0.83	0.81	0.77	0.72						
15	1.88	0.77	0.74	0.95	0.9	0.79	0.8						
5	7.9	0.74	0.82	0.96	0.68	0.76	0.74						
	90	105	120	135	150	165	180	195	210	225	240	255	270

Table A8
η R-08-20.

50	0	0	0	0	0.63	0.71	0.73						
45	0	0	0.9	0.75	0.74	0.65	0.68						
35	0	0.88	0.73	0.78	0.71	0.81	0.81						
25	21.55	0.93	0.79	0.64	0.76	0.77	0.69						
15	43.30	0.96	0.67	0.89	0.95	0.83	0.83						
5	59.03	1.26	0.93	0.99	0.69	0.83	0.95						
	90	105	120	135	150	165	180	195	210	225	240	255	270

Table A9
η R-08-30.

50	0	0	0	0	0.67	0.72	0.72						
45	0	0	1.01	0.78	0.74	0.65	0.68						
35	0	1.5	0.73	0.78	0.71	0.82	0.74						
25	51.91	0.93	0.79	0.79	0.84	0.77	0.69						
15	43.30	1.35	0.88	0.89	0.95	0.83	0.83						
5	92.59	1.26	0.93	0.99	0.67	0.86	0.84						
	90	105	120	135	150	165	180	195	210	225	240	255	270

Table A10
η R-08-40.

50	0	0	0	0	0.70	0.70	0.83						
45	0	0	1.02	0.8	0.74	0.65	0.68						
35	0	1.73	0.73	0.78	0.71	0.72	0.62						
25	84.34	0.93	0.79	0.82	0.71	0.77	0.69						
15	43.30	1.76	0.95	0.89	0.95	0.83	0.83						
5	151.72	1.26	0.93	0.99	0.61	0.69	0.64						
	90	105	120	135	150	165	180	195	210	225	240	255	270

Table A11
η R-07-20.

50	0	0	0	0	0.56	0.63	0.73						
45	0	0	0.77	0.69	0.74	0.65	0.68						
35	0	0.87	0.83	0.74	0.74	0.80	0.80						
25	30.82	0.81	0.81	0.63	0.76	0.75	0.67						
15	32.20	1.14	0.66	0.87	0.83	0.82	0.82						
5	51.65	1.19	1.11	0.95	0.68	0.83	0.92						
	90	105	120	135	150	165	180	195	210	225	240	255	270

Table A12
η R-07-30.

50	0	0	0	0	0.59	0.67	0.70						
45	0	0	0.76	0.71	0.69	0.65	0.66						
35	0	1.27	0.80	0.76	0.68	0.75	0.74						
25	35.85	1.11	0.95	0.65	0.69	0.69	0.59						
15	61.17	1.51	0.79	0.94	0.75	0.77	0.77						
5	100.31	1.42	0.97	0.90	0.60	0.72	0.81						
	90	105	120	135	150	165	180	195	210	225	240	255	270

Table A13
η R-07-40.

50	0	0	0	0	0.66	0.72	0.64						
45	0	0	1.22	0.82	0.69	0.65	0.66						
35	0	1.75	0.8	0.76	0.68	0.69	0.63						
25	83.04	1.11	0.95	0.81	0.72	0.69	0.59						
15	61.17	1.9	0.94	0.94	0.75	0.77	0.77						
5	157.44	1.42	0.97	0.90	0.61	0.65	0.64						
	90	105	120	135	150	165	180	195	210	225	240	255	270

Table A14
η R-06-20.

50	0	0	0	0	0.59	0.67	0.71						
45	0	0	0.65	0.67	0.65	0.65	0.70						
35	0	0.86	0.78	0.73	0.69	0.79	0.78						
25	25.13	1.01	0.76	0.64	0.73	0.72	0.65						
15	25.47	0.97	0.68	1.02	0.92	0.80	0.85						
5	63.86	1.07	0.89	0.66	0.71	0.84	0.87						
	90	105	120	135	150	165	180	195	210	225	240	255	270

Table A15
η R-06-30.

50	0	0	0	0	0.58	0.61	0.67						
45	0	0	0.83	0.71	0.61	0.61	0.65						
35	0	1.26	0.86	0.68	0.61	0.71	0.74						
25	40.57	1.39	0.84	0.63	0.68	0.68	0.62						
15	51.29	1.33	0.75	0.91	0.79	0.72	0.80						
5	101.47	1.52	0.99	0.88	0.65	0.73	0.80						
	90	105	120	135	150	165	180	195	210	225	240	255	270

Table A16
η R-06-40.

50	0	0	0	0	0.60	0.58	0.56						
45	0	0	0.88	0.77	0.70	0.54	0.51						
35	0	1.60	0.87	0.80	0.64	0.61	0.58						
25	62.59	1.53	0.97	0.69	0.64	0.60	0.43						
15	80.32	2.02	0,90	0.97	0.81	0.58	0.64						
5	167.97	2.31	0.99	0.87	0.58	0.56	0.56						
	90	105	120	135	150	165	180	195	210	225	240	255	270

Table A17
η R-05-20.

50	0	0	0	0	0.52	0.64	0.67						
45	0	0	0.95	0.71	0.62	0.56	0.59						
35	0	1.12	0.81	0.67	0.65	0.65	0.67						
25	25.2	0.81	0.72	0.67	0.70	0.69	0.62						
15	24.67	0.92	0.67	0.90	0.81	0.75	0.86						
5	61.54	1.19	0.83	0.90	0.72	0.82	0.84						
	90	105	120	135	150	165	180	195	210	225	240	255	270

Table A18
η R-05-30.

50	0	0	0	0	0.57	0.57	0.63						
45	0	0	0.65	0.66	0.63	0.65	0.66						
35	0	0.79	0.85	0.70	0.69	0.75	0.75						
25	37.56	1.30	0.70	0.63	0.66	0.69	0.59						
15	39.88	1.35	0.8	0.99	0.79	0.65	0.79						
5	111.03	1.71	1.08	0.89	0.65	0.75	0.78						
	90	105	120	135	150	165	180	195	210	225	240	255	270

Table A19
η R-05-40.

50	0	0	0	0	0.59	0.55	0.54						
45	0	0	0.87	0.74	0.69	0.52	0.52						
35	0	1.49	0.94	0.77	0.66	0.58	0.52						
25	48.8	1.65	0.9	0.69	0.64	0.52	0.45						
15	56.71	1.94	0.96	0.98	0.78	0.54	0.64						
5	168.92	2.12	1.00	0.92	0.6	0.55	0.54						
	90	105	120	135	150	165	180	195	210	225	240	255	270

Appendix B. Standard daylight characteristic of LCP configuration for diffuse vertical illuminance *ηdiffuse(T-R)* = *Ediffuse(T-R)/Ediffuse(ZERO)*

See Table B1.

Table B1
ηdifusef(T-R).

LCP configurations	η
BaseCase	0.85
T-05-17	0.93
T-05-22	1.00
T-05-27	1.06
T-06-17	1.00
T-06-22	1.07
T-06-27	1.12
R-08-20	0.83
R-08-30	0.86
R-80-40	0.88
R-07-20	0.84
R-07-30	0.87
R-07-40	0.88
R-06-20	0.82
R-06-30	0.85
R-06-40	0.87
R-05-20	0.81
R-05-30	0.85
R-05-40	0.87

Appendix C. Parametric laboratory study at the daylight laboratory at NTNU

See Figs. C1–C5.

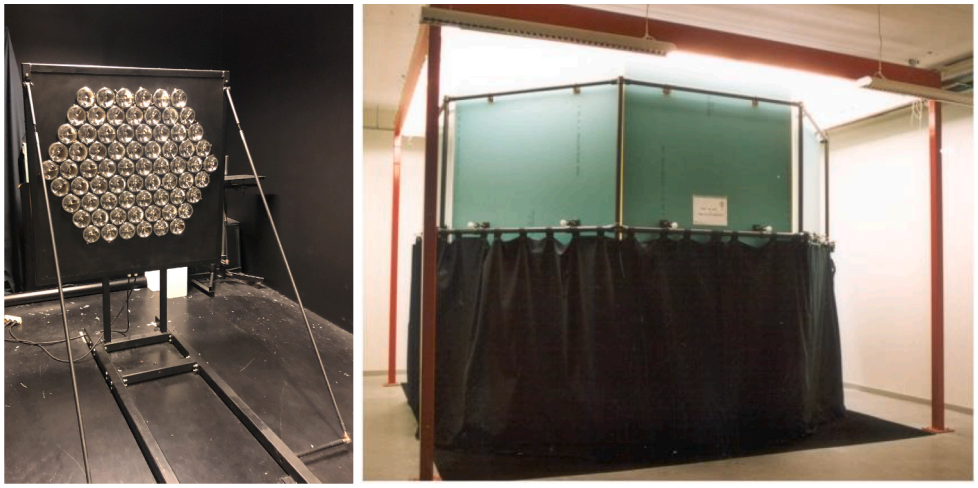

Fig. C1. (Left) Artificial sun composed of 70 halogen lamps with parabolic reflectors (50 W) fixed to a vertical metal plate and arranged in a hexagonal pattern; (right) artificial overcast sky in the form of octagonal mirror box.

Fig. C2. Model setup in the laboratory study with direct light (left) and diffuse light (right).

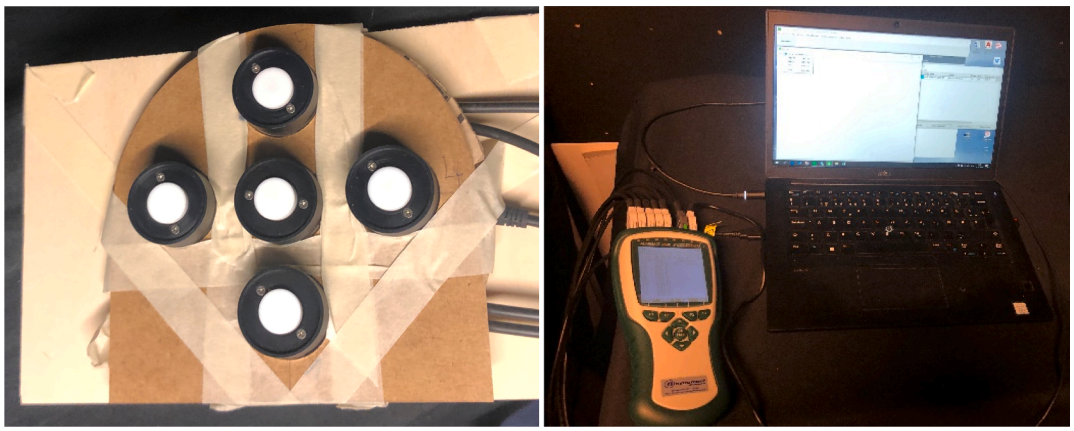

Fig. C3. (left) Measurement instrument Almemo Ahlborn, with photosensors fixed on a circular plate and placed at the tube's exit; (right) logging of measuring data via Ahlborn Almemo logger and Almemo control 6.0 software.

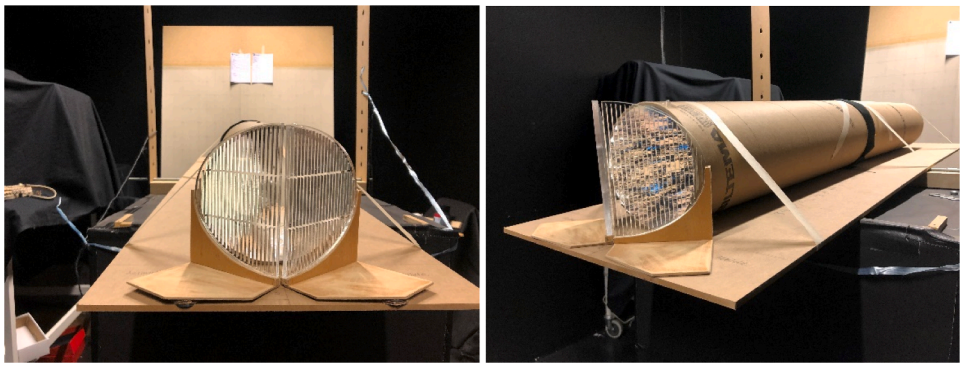

Fig. C4. Laser-Cut panel T sample for tilt probe.

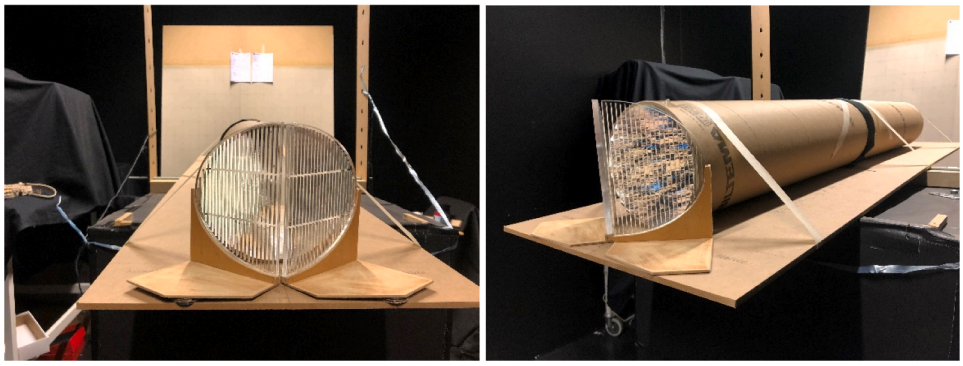

Fig. C5. Laser-Cut panel R sample for rotated probe.

Appendix D. Uniformity of the direct light from the artificial sun at the daylight laboratory at NTNU

See Table D1.

Table D1
Uniformity of the direct light from the artificial sun for the direct light experimental test.

Altitude							
50°					0.93	0.95	0.95
45°				0.92	0.94	0.97	0.96
35°		0.85	0.91	0.94	0.96	0.97	0.97
25°		0.89	0.93	0.96	0.97	0.97	0.98
15°		0.88	0.95	0.96	0.94	0.98	0.98
5°		0.89	0.99	0.96	0.98	0.97	0.98
Azimuth	90°	105°	120°	135°	150°	165°	180°

References

Arnesen, H., Kolås, T., Matusiak, B., 2011. A guide to dayligthting and solar shading systems at high latitude. The research Center on Zero Emission Buildings (ZEB) - Project Report 3, Oslo, Norway.

Chinazzo, G., Chamilothori, K., Wienold, J., Andersen, M., 2020. Temperature-color interaction: subjective indoor environmental perception and physiological responses in virtual reality. Hum. Fact.

Christoffersen, J., Johnsen, K., 1999. Vinduer og dagslys-en feltundersøgelse i kontorbygninger.

Courret, G., Scartezzini, J.-L., Francioli, D., Meyer, J.-J., 1998. Design and assessment of an anidolic light-duct. Energy Build. 28 (1), 79–99.

Creda, P.J., Matusiak, B.S., 2017. Toward new design of laser cut panels for scattering of sunlight at high latitudes, Passive Low Energy Architecture, PLEA. In: PLEA Conference, Edinburg.

Edmonds, I., 2005. Daylighting high-density residential buildings with light redirecting panels. Light. Res. Technol. 37 (1), 73–84.

Edmonds, I., Moore, G., Smith, G., Swift, P., 1995. Daylighting enhancement with light pipes coupled to laser-cut light-deflecting panels. Int. J. Light. Res. Technol. 27 (1), 27–35.

Edmonds, I., Pearce, D., 1999. Enhancement of crop illuminance in high latitude greenhouses with laser-cut panel glazing. Sol. Energy 66 (4), 255–265.

Edmonds, I.R., 1993. Performance of laser cut light deflecting panels in daylighting applications. Sol. Energy Mater. Sol. Cells 29 (1), 1–26.

Freewan, A.A., 2014. Maximizing the performance of laser cut panel by interaction of ceiling geometries and different aspect ratio. J. Daylight. 1 (1), 29–35.

Galasiu, A.D., Atif, M.R., MacDonald, R.A.J.S.E., 2004. Impact of window blinds on daylight-linked dimming and automatic on/off lighting controls. Sol. Energy 76 (5), 523–544.

Garcia-Hansen, V., Edmonds, I., 2015. Methods for the illumination of multilevel buildings with vertical light pipes. Sol. Energy 117, 74–88.

Garcia Hansen, V., Edmonds, I., 2003. Natural illumination of deep-plan office buildings: light pipe strategies. In: Proceedings of ISES Solar World Congress. Gothenburg, Sweden.

Garcia Hansen, V., Edmonds, I., Bell, J., 2009. Improving daylighting performance of mirrored light pipes. In: PLEA2009 - 26th Conference on Passive and Low Energy Architecture. Quebec City, Canada.

Garcia Hansen, V., Edmonds, I., Hyde, R., 2001. The use of light pipes for deep plan office buildings: a case study of Ken Yeang's bioclimatic skyscraper proposal for KLCC, Malaysia.

Google, 2019. Climate and temperature in Oslo (accessed december 2019).

Herring, H.J.E., 2006. Energy efficiency—a critical view. 31(1), 10–20.

Houck, L.D., 2015. A novel approach on assessing daylight access in schools. Procedia Econ. Fin. 21, 40–47.

Johnsen, K., Christoffersen, J., Sørensen, H., Jessen, G., 2011. Integreret regulering af solafskærmning, dagslys og kunstlys. SBi 2011 (15), 112.

Kadir, A.A., Ismail, L.H., Kasim, N., Wahab, I.A., Kaamin, M., binti Ngadiman, N., Rosli, M.S.B.M., 2019. Improving the performance of light pipe system using laser cut panel. In: Journal of Physics: Conference Series. IOP Publishing, p. 012064.

Kischkoweit-Lopin, M., 2002. An overview of daylighting systems. Sol. Energy 73 (2), 77–82.

Knoop, M., Aktuna, B., Bueno, B., Darula, S., Deneyer, A., Diakite, A., Fuhrmann, P., Geisler-Moroder, D., Hubschneider, C., Johnsen, K., 2016. Daylighting and Electric Lighting Retrofit Solutions. Universitätsverlag der TU Berlin.

Kolås, T., 2011. LECO–Energy Efficient Lighting: Technologies and Solutions for Significant Energy Savings Compared to Current Practice in Norwegian Office Buildings. SINTEF Building and Infrastructure.

Kolås, T., 2013. Performance of Daylight Redirecting Venetian Blinds for Sidelighted Spaces at High Latitudes. The Norwegian Institute of Technology, Trondheim, Norway.

Kottek, M., Grieser, J., Beck, C., Rudolf, B., Rubel, F., 2006. World map of the Köppen-Geiger climate classification updated. Meteorol. Z 15 (3), 259–263.

Kwok, C., Chung, T., 2008. Computer simulation study of a horizontal light pipe integrated with laser cut panels in a dense urban environment. Light. Res. Technol. 40 (4), 287–305.

l'Eclairage, C.I.d., 2006. Tubular daylight guidance systems. CIE Technical report 173: 2006. Commission Internationale de l'Eclairage. CIE, Vienna.

Labib, R., 2013. Improving daylighting in existing classrooms using laser cut panels. Light. Res. Technol. 45 (5), 585–598.

Lindberg, K.B., Bakker, S.J., Sartori, I., 2019. Modelling electric and heat load profiles of non-residential buildings for use in long-term aggregate load forecasts. Utilit. Policy 58, 63–88.

Lindsay, C., Littlefair, P., 1992. Occupant use of venetian blinds in offices. Building research establishment.

Lynes, J., Gilding, A., 2000. Parallax in artificial sky domes. Int. J. Light. Res. Technol. 32 (3), 157–160.

Mardaljevic, J., Christoffersen, J., Raynham, P., 2013. A proposal for a European standard for daylight in buildings. In: Proc. Int. Conf. Lux Europa, pp. 237–250.

Matusiak, B., Arnesen, H., 2005. The limits of the mirror box concept as an overcast sky simulator. Light. Res. Technol. 37 (4), 313–327.

Matusiak, B.S., Braczkowski, T., 2014. Overcast sky simulator in the Daylight laboratory at NTNU, Trondheim. Lumen V4.

Mayhoub, M.S., 2011. Hybrid Lighting Systems: Performance, Application and Evaluation. University of Liverpool.

Nair, M., Ganesan, A., Ramamurthy, K., 2015. Daylight enhancement using laser cut panels integrated with a profiled Fresnel collector. Light. Res. Technol. 47 (8), 1017–1028.

Obradovic, B., Matusiak, B.S., 2019. Daylight transport systems for buildings at high latitudes. J. Daylight. 6 (2), 60–79.

Perez, O.L., Strother, C., Vincent, R., Rabin, B., Kaplan, H., 2018. Effects of 'Blue-Regulated' full spectrum LED lighting in clinician wellness and performance, and patient safety. In: Congress of the International Ergonomics Association. Springer, pp. 667–682.

Rea, M.S., 1984. Window blind occlusion: a pilot study. Build. Environ. 19 (2), 133–137.

Reinhart, C.F., 2004. Lightswitch-2002: a model for manual and automated control of electric lighting and blinds. Sol. Energy 77 (1), 15–28.

Rubin, A.I., Collins, B.L., Tibbott, R.L., 1978. Window Blinds as a Potential Energy Saver: A Case Study. US Department of Commerce, National Bureau of Standards.

Ruck, N., Aschehoug, O., Aydinli, S., Christoffersen, J., Edmonds, I., Jakobiak, R., Kischkoweit-Lopin, M., Klinger, M., Lee, E., Courret, G., 2000. Daylight in Buildings-A Source Book on Daylighting Systems and Components. Lawrence Berkeley National Laboratory, Berkeley (USA).

Satel-Light, 1998. Satel-Light Database for Oslo, Norway (accessed May 2019).

Satel-Light. Satel-Light data, Illuminance on a vertical south oriented surface, Oslo, Norway, 2019.

SRML, U.o.O., 2019. Solar Chart http://solardat.uoregon.edu/SunChartProgram.html (accessed december 2019).

Ulimoen, I., Karlsen, L., Bottheim, R.M., Drolsum Roekenes, H., Marini, A., 2020. Dagslys i bygninger. Rådgivende Ingeniørers Forening RIF, https://www.rif.no/.

Venturi, L., Wilson, M., Jacobs, A., Solomon, J., 2006. Light piping performance enhancement using a deflecting sheet. Light. Res. Technol. 38 (2), 167–179.

Wadsworth, F.L.O., 1903. Illuminating glass plate, in: Office, U.S.P. (Ed.).

Weibye, A., Matusiak, B., 2019. Towards new design of laser cut acrylic panels for windows. J. Daylight. 6 (1), 1–10.

Yeang, K., Powell, R., 2007. Designing the ecoskyscraper: premises for tall building design. Struct. Design Tall Special Build. 16 (4), 411–427.

Yuda, E., Ogasawara, H., Yoshida, Y., Hayano, J.J., 2017. Exposure to blue light during lunch break: effects on autonomic arousal and behavioral alertness. 36(1), 30.

Zastrow, A., Wittwer, V., 1986. Daylighting with fluorescent concentrators and highly reflective silver-coated plastic films: a new application for new materials. In: Optical Materials Technology for Energy Efficiency and Solar Energy Conversion V. International Society for Optics and Photonics, Innsbruck, Austria, pp. 93–101.

Zastrow, A., Wittwer, V., 1987. Daylighting with mirror light pipes and with fluorescent planar concentrators. In: First Results from the Demonstration Project Stuttgart-Hohenheim, Materials and Optics for Solar Energy Conversion and Advanced Lightning Technology. International Society for Optics and Photonics, San Diego, United States, pp. 227–235.